

Katharina Schmölzer

**Process Engineering
to Overcome Substrate and Product
Toxicity in *E. coli* Whole Cell-catalyzed
Reduction of *o*-Chloroacetophenone**

Diplomarbeit

zur Erlangung des akademischen Grades einer
Diplom-Ingenieurin

der Studienrichtung Biotechnologie
erreicht an der

Technischen Universität Graz

Betreuer:

Univ. Prof. Dipl.-Ing. Dr. Bernd Nidetzky

Dipl.-Ing. Dr. Regina Kratzer

Institut für Biotechnologie und Bioprozesstechnik

Technische Universität Graz

2010

EIDESSTATTLICHE ERKLÄRUNG

Ich erkläre an Eides statt, dass ich die vorliegende Arbeit selbstständig verfasst, andere als die angegebenen Quellen/Hilfsmittel nicht benutzt, und die den benutzten Quellen wörtlich und inhaltlich entnommene Stellen als solche kenntlich gemacht habe.

Graz, am

.....

(Unterschrift)

STATUTORY DECLARATION

I declare that I have authored this thesis independently, that I have not used other than the declared sources / resources, and that I have explicitly marked all material which has been quoted either literally or by content from the used sources.

.....

date

.....

(signature)

Acknowledgement

I would like to express my appreciation to my supervisor Univ.-Prof. Dipl.-Ing. Dr. Bernd Nidetzky. Thanks for giving me the opportunity to be part of this research group.

Special thanks go to Dipl.-Ing. Dr. Regina Kratzer, for her time, patience, and understanding.

Also, thanks to the members of the Institute of Biotechnology and Biochemical Engineering.

I dedicate this thesis to my boyfriend and my parents who unremittingly supported me during my years of study. They made this work possible.

Kurzfassung

Bioreduktion von *o*-Chloroacetophenon ist die bevorzugte Methode zur Herstellung von 1-(2-chlorophenyl)ethanol, der chiralen Schlüsselverbindung zur Synthese einer neuen Klasse von chemotherapeutischen Substanzen. Die ausgeprägte Toxizität von Substrat und Produkt limitiert allerdings Ausbeute sowie Produktivität durch rasche Deaktivierung des Katalysators in Ganzzell-katalysierten Reduktionen. Die Halbwertszeit eines für die NADH-abhängige *o*-Chloroacetophenon Reduktion konstruierten *E.coli* Stamms beträgt in Gegenwart von 100 mM Substrat nur 20 Minuten. Durch systematische Prozess- und Reaktionsoptimierungen konnte die Ausbeute der *E.coli* katalysierten Reduktion von *o*-Chloroacetophenon zum entsprechenden Alkohol verbessert werden. Insbesondere Fed-batch Strategien sowie *in situ* Substratzugabe und Produktextraktion mit nicht mischbaren Lösungsmitteln oder hydrophoben Trägermaterialien eignen sich zur Verringerung der Konzentration toxischen Substrats und Produkts in der wässrigen Phase. Strukturierte Reaktionsoptimierung hinsichtlich Art und Menge von polymeren Trägermaterialien oder mit Wasser nicht mischbaren Lösungsmitteln mit gleichzeitiger Optimierung des pH-Wertes bewirkte eine Steigerung der Ausbeute um das 18-fache. Höchste Produktivitäten erzielten mit Polymyxin B Sulfat (36 μ M) permeabilisierte Zellen durch die Zugabe von 20 vol% Hexan und 500 μ M NAD⁺ und einem Prozess pH von 6.2. Unter optimierten Bedingungen konnten 300 mM *o*-Chloroacetophenon mit einer analytischen und isolierten Ausbeute von 95 und 88 %, beziehungsweise mit einer Gesamtausbeute von 0,62 g, umgesetzt werden.

Schlüsselworte: asymmetrische Katalyse; *E. coli*; *in situ* Produktentfernung; organisches Co-Lösungsmittel; polymeres Adsorbent; Reduktion

Abstract

Bioreduction of *o*-chloroacetophenone is the preferred method of 1-(2-chlorophenyl)ethanol production, the chiral key intermediate in the synthesis of a new class of chemotherapeutic substances. The pronounced toxicity of substrate and product limited productivity and product yield by fast catalyst deactivation in whole cell catalyzed reductions. The half-life time of an *E. coli* designed for NADH-dependent *o*-chloroacetophenone reduction was determined to 20 min in the presence of 100 mM substrate. Systematic process and reaction optimization was used to enhance the product yield of *E. coli* catalyzed reduction of *o*-chloroacetophenone to the corresponding Prelog-alcohol. The concentrations of substrate and product in the catalyst-containing, aqueous phase were reduced by fed-batch strategies and *in situ* substrate supply and product removal. Reaction optimization with respect to type and amount of *in situ* extracting polymeric hydrophobic resins or water-immiscible co-solvents with subsequent identification of optimal pH caused an up to 18-fold increase in yield. Application of 20% (v/v) hexane as co-solvent at pH 6.2 and supplementation of external NAD⁺ (500 μM) to cells permeabilized with polymyxin B sulphate (36 μM) was most effective in enhancing product yield. Under optimized conditions, 300 mM of *o*-chloroacetophenone were reduced with analytical and isolated yields of 95 and 88 %, respectively in a total yield of 0.62 g.

Keywords: asymmetric catalysis; *E. coli*; *in situ* product removal; organic co-solvent; polymeric adsorbent; reduction

Contents

MAIN PART	9
1. Introduction	9
2. Results and Discussion	12
2.1. Batch and Fed-batch Experiments	12
2.2. Substrate and Product “Toxicity”	13
2.3. In Situ Substrate Supply (ISSS) and Product Removal (ISPR)	15
2.3.1. ISSS and ISPR by a Resin	15
2.3.2. ISSS and ISPR by Organic Co-solvents	19
2.4. Effect of Different <i>E.coli</i> Strains	24
2.5. Effect of pH	25
2.6. Scale-up and Downstream-processing	29
3. Conclusions	31
4. Experimental Section	32
4.1. Chemicals, Materials and Strains	32
4.2. Cultivation of Strains	33
4.3. Enzyme Activity Measurements in the Cell-free Extracts	33
4.4. Evaluation of Substrate and Product “Toxicity”	34
4.5. Whole-cell Bioreduction of <i>o</i> -Chloroacetophenone	34
4.6. Analytical Methods	36
5. References	38
APPENDIX	41
A. Introduction	41
A.1. Polo-like Kinase 1 (PLK 1) Inhibitors	41
B. Results and Discussion	42
B.1. Substrate and Product “Toxicity”	42
B.2. Effect of Different <i>E. coli</i> Strains	52
B.3. Effect of pH	55
B.3.1. ISSS and ISPR by a Resin	55
B.3.2. ISSS and ISPR by Hexane	56
B.3.3. Substrate Toxicity at Different pH-values	58
B.4. Alternatives for Downstream-processing	60

B.5. NMR Spectra	62
C. Registers.....	64
C.1. Register of Figures.....	64
C.2. Register of Schemes	72
C.3. Register of Tables.....	73
D. References Appendix	74

Process Engineering to Overcome Substrate and Product Toxicity in *E. coli* Whole Cell-catalyzed Reduction of *o*-Chloroacetophenone

Regina Kratzer^{a,*}, Katharina Schmölder^a, Katharina Mädje^a, and Bernd Nidetzky^{a,*}

^a Institute of Biotechnology and Biochemical Engineering, Graz University of Technology, Petersgasse 12, A-8010 Graz, Austria

Fax: (+43)-(0)316-873-8434; phone: (+43)-(0)316-873-8408 (Regina Kratzer); (+43)-(0)316-873-8400 (Bernd Nidetzky); e-mail: regina.kratzer@tugraz.at;

bernd.nidetzky@tugraz.at

In preparation for Advanced Synthesis & Catalysis.

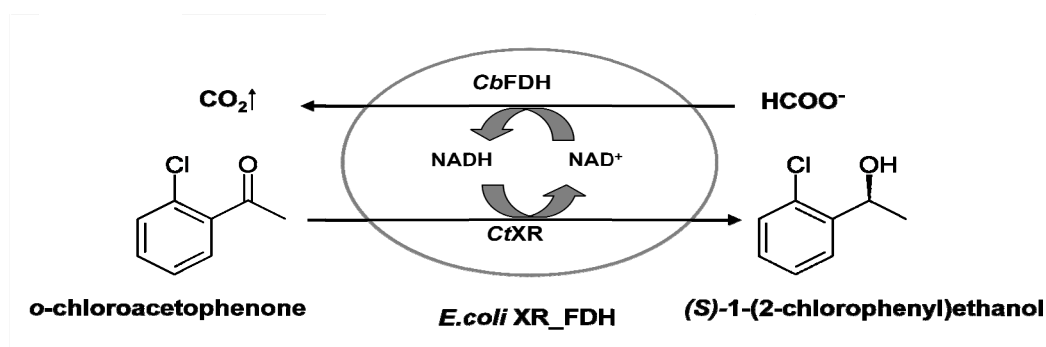
MAIN PART

1. Introduction

The integration of enzyme catalyzed reactions into multi-step synthesis routes has become increasingly common in the manufacture of enantiomerically pure pharmaceuticals. Enzymatic production of chiral key intermediates in exquisite stereoselectivities and without the need of protection-deprotection strategies has an enormous potential to simplify pharmaceutical processes. Bottlenecks in interfacing biocatalysis and organic synthesis are

generally biocatalyst stability, solvent incompatibility, product/substrate solubility and product recovery. The investigation and identification of limiting factors in the enzymatic step is of prime importance in the early phase of development and can lead to dramatically increased process improvements. Secondary alcohols are frequently used as chiral key intermediates and their preparation by asymmetric reduction of a precursor ketone is generally preferred to resolution of a racemic mixture of alcohols. The lack of universally applicable asymmetric hydrogen donors requires case-specific optimization of the reduction step in newly discovered active pharmaceutical compounds. Inhibitors of polo-like kinase 1 (PLK1) have recently shown good antitumor efficacy in xenograft tumor models.^[1,2] Thiophene-benzimidazole and -imidazopyridine are currently among the most promising PLK1 inhibitor candidates and *S*-1-(*o*-chlorophenyl)-ethanol is used as chiral key intermediate in their synthesis.^[2,3,4] A wide range of chemo- and enzymatic catalysts have been explored for asymmetric *o*-chloroacetophenone reduction. However, except for very few examples, use of these catalysts was prohibited by insufficient enantioselectivity and/or low productivities.^[5,6,7] *Candida tenuis* xylose reductase is among the very few reductases capable of *o*-chloroacetophenone reduction in absolute stereoselectivity (> 99 % ee) and useful activity. The enzyme provides the additional convenience of a detailed structural and kinetic characterization, a prerequisite for subsequent reaction engineering. However, the sparingly water soluble *o*-chloroacetophenone turned out as highly toxic to the isolated enzyme at concentrations above its solubility limit of ≥ 0.15 g/L. Development of a whole cell catalyst by co-expression of CtXR and *Candida boidinii* formate dehydrogenase in *E. coli* stabilized the enzymes in the cellular environment and minimized the steps of biocatalyst preparation.^[8] NADH-recycling by the oxidation of formate keeps a high redox economy while producing volatile CO₂ as only by-product (Scheme 1). However, *o*-chloroacetophenone was still highly

toxic to the whole cell biocatalyst, restricting the yield of batch processes with 100 mM substrate to maximally 16%. We have previously shown that the regime of catalyst inactivation was (partly) alleviated by enhancing the activity of *E. coli* cells using permeabilization and cofactor supplementation.^[8] Here, we have systematically investigated substrate and product toxicities on catalyst life-time and productivities. The results guided the controlled supply and removal of toxic compounds from the aqueous phase by *in situ* substrate supply and product removal via polymeric adsorbent resins and water immiscible second phases. We furthermore studied the impact of engineering strategies to protect the catalyst on downstream processing, an issue that is often neglected. Our investigations uncover limitations in whole cell bioreductions and provide methods to (partly) overcome substrate and product “toxicity”. Catalyst instability is often encountered in biocatalysis and strategies to (partly) overcome the problems will be a useful guide to other workers in the field.



Scheme 1. Whole-cell biocatalytic reduction of *o*-chloroacetophenone using recombinant *E. coli* strains co-expressing *Candida tenuis* xylose reductase (*CtxR*) and *Candida boidinii* formate dehydrogenase (*CbFDH*).

2. Results and Discussion

2.1. Batch and Fed-batch Experiments

We previously reported the development of an *E. coli* whole cell catalyst based on co-expression of *Candida tenuis* xylose reductase (XR) and *Candida boidinii* formate dehydrogenase (FDH). Time courses of 100 mM *o*-chloroacetophenone reduction were characterized by a sharp decrease in the conversion rate which occurred at approximately the same time during the initial phase of the transformation. A catalyst half-life time of 20 min was determined in the presence of 100 mM substrate.^[9] Since controlled supply of toxic substrates can prolong catalyst life-time, we chose fed-batch addition of *o*-chloroacetophenone to alleviate toxic effects of the aromatic ketone on *E. coli* cells.^[10,11,12] Table 1 compares yields of batch and fed-batch conversions varying substrate end-concentrations and feeding rates. Catalyst productivities in batch conversions were ~ 0.45 g/g irrespective of a substrate concentration between 30 to 60 mM. Highest conversion of 47 % was therefore obtained with 30 mM *o*-chloroacetophenone. Slow addition of substrate increased productivities between 1.2-2.7-fold. Maximal productivity improvement between batch and fed-batch conversion was obtained with a total substrate concentration of 50 mM and a feeding rate of 10 mM/60 min. Clearly, the fed-batch strategy contributed to the desired improvement in the product titer and more importantly, could be applied conveniently. However, sequential addition of the substrate showed little enhancement in the final product concentration indicating inhibition or toxicity of the product 1-(2-chlorophenyl)ethanol to engineered *E. coli* cells. A detailed study of the dependence of catalyst life-time on *o*-chloroacetophenone and 1-(2-chlorophenyl)ethanol concentrations can guide further *in situ*

substrate supply and product removal strategies. We therefore determined catalyst stability in the presence of different substrate or product concentrations.

Table 1. Effect of substrate (end)-concentration and feeding rate on yields in batch and fed-batch conversions of *o*-chloroacetophenone with *E. coli* BL21 (DE3) pETDuet1_XR_FDH. ^{a)}

CDW [g/L] ^{b)}	Feed-Rate	<i>o</i> -chloroacetophenone [mM]	Yield [g/g]	Yield [%]
30.6	Batch	50	9.0	17
43.0	Batch	60	10.6	18
42.1	Batch	30	14.2	47
38.1	Batch	50	12.0	24
30.6	10mM/60min	50	24.5	49
43.0	3mM/20min	60	17.9	30
42.1	3mM/40min	30	17.4	58
38.1	5mM/40min	50	18.8	38

^{a)}Reaction conditions: whole cell biocatalyst, reaction-time 300 to 400 minutes; pH 7.5, 30°C, 30 rpm.

^{b)} CDW = cell dry weight (cell dry weight between 30 and 40 g/L).

2.2. Substrate and Product “Toxicity”

We incubated *E. coli* biomass in the presence of substrate or product identically as in batch conversions and measured loss of relevant enzyme activities in dependence of incubation time. Table 2 shows calculated half-life times of XR and FDH in the presence of 0-50 mM *o*-chloroacetophenone or 1-(2-chlorophenyl)ethanol. The half-life times of XR and FDH in buffer were determined to 5 and 8 d, respectively, but decreased to 4-11 % at substrate- or product-concentrations of 10 mM. Half-life times of catalytic activities in *E. coli* XR_FD

cells further decreased to ~1 h at 30 mM substrate or product. The presence of 50 mM 1-(2-chlorophenyl)ethanol had a strong negative impact on the stabilities of XR and FDH and a catalyst half-life time of only 10 min was measured. Accumulation of the highly toxic product provides the explanation for the only moderate increases in productivity in fed-batch compared to batch conversions.

Table 2. Half-life of the enzymes XR and FDH in the presence of different substrate and product concentrations.^{a)}

Conc. [mM]	<i>o</i> -chloroacetophenone		<i>(S)</i> -1-(2-chlorophenyl)ethanol	
	T _{1/2} XR [min]	T _{1/2} FDH [min]	T _{1/2} XR [min]	T _{1/2} FDH [min]
0	6931	11552	6931	11552
3	6931	7702	n.d.	n.d.
6	3466	6931	n.d.	n.d.
10	770	495	330	990
20	112	173	248	239
30	71	67	49	53
40	n.d.	n.d.	21	16
50	51	65	10	10

^{a)} Reaction conditions: *E. coli* BL21 (DE3) pETDuet1_XR_FDH (whole cell biocatalyst); [cells] = 40 g_{CDW}/L; pH 7.5; 30°C; 30 rpm.

2.3. In Situ Substrate Supply (ISSS) and Product Removal (ISPR)

High toxicity of product and substrate required separation of catalyst from high substrate and product concentrations. To prolong catalyst life-time and hence productivity in whole cell bioreductions substrate and product concentration should not exceed 3 mM in the catalyst containing aqueous phase. We chose two alternatives for ISSS and ISPR: (a) immobilization via adsorption onto polymeric matrices, and (b) extraction into a second organic phase. These are elegant methods to decrease the concentration of toxic substrates and products in the aqueous phase.^[10,11] Key parameters of suitable second phases are biocompatibilities and distribution ratio of the reactants between the second phase and the aqueous phase.

2.3.1. ISSS and ISPR by a Resin

Adsorbent resins have been reported to alleviate substrate and product inhibition or toxicity and facilitate product recovery in biocatalysis.^[11] Selected resins can overcome disadvantages of traditional organic solvents such as poor biocompatibility, volatilization and environmental hazard. To understand the principle of using polymeric adsorbent resins for in situ extractions, it is helpful to think of them as “solid organic solvents”, however, instead of removing the product/substrate from the reaction mixture by extraction into a liquid organic phase, the product/substrate is removed via adsorption onto the high surface area of a solid organic phase. The driving force for the adsorption is the interaction between the nonpolar regions of the adsorbed molecule with the nonpolar polymeric resin surface.^[11]

We used the polymeric adsorbent AMBERLITE™ XAD7HP from Rohm and Haas, supplied as white insoluble beads. The non ionic, aliphatic and acrylic polymer derives its adsorptive properties from its patented macroreticular structure (containing both a continuous polymer phase and a continuous pore phase), high surface area and the aliphatic nature of its surface. The ability to adsorb non polar compounds from aqueous systems as well as polar compounds from non-polar solvents is ascribed to its aliphatic character.^[13]

The resin's adsorption capacity for *o*-chloroacetophenone and 1-(2-chlorophenyl)ethanol was tested in preliminary binding studies. A ratio of 100 mM substrate or product to 20 vol% resin kept the effective substrate or product concentration in the aqueous phase below 3 mM. Control experiments indicated synergistic effects of substrate and product binding; mixing of 50 mM substrate, 50 mM product and 20 vol% resin resulted in 3 mM product and 2 mM substrate in the aqueous phase. As a result of this we used higher resin amounts for our bioprocess.

Figure 1 and 2 show time courses of resin-based whole cell bioreductions varying substrate and resin concentrations. Highest product concentration was obtained with 100 mM *o*-chloroacetophenone and 30 vol% resin after a reaction time of 24 h. The analytical yield amounted to 86 mM with a respective conversion of 86 %. Reduced yields in experiments with resin concentrations > 30 vol% suggest too low substrate concentrations in the aqueous phase. By doubling the concentrations of resin and substrate of the best experiment we kept the optimal substrate to resin ratio, however insufficient stirring of the highly viscous reaction mixture resulted in low yield.

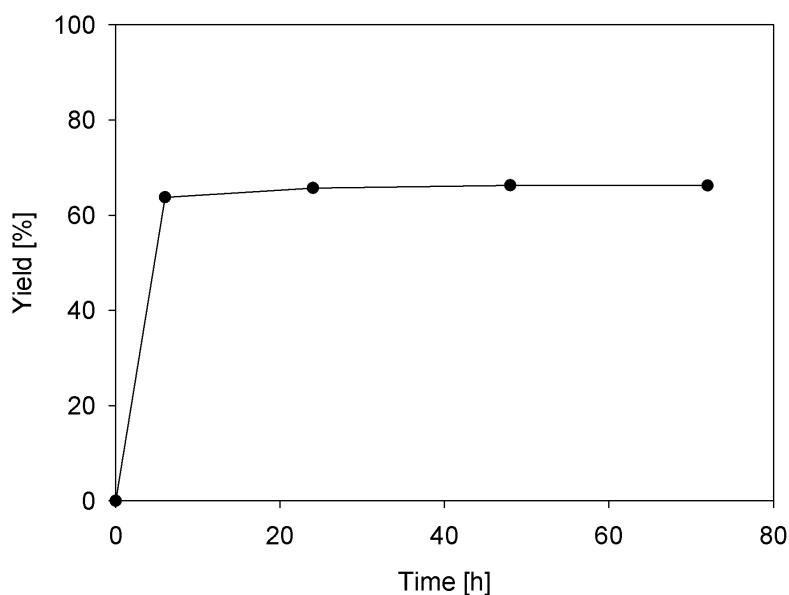


Figure 1. Time course of resin-based whole cell bioreductions using 100 mM substrate and 20 vol% resin. Conditions: *E. coli* BL21 (DE3) pETDuet1_XR_FDHD (whole cells); [cells] = 40 g_{CDW}/L; pH 7.5; 30°C; 30 rpm. Symbols: ● = 100 mM *o*-chloroacetophenone + 20 vol% resin.

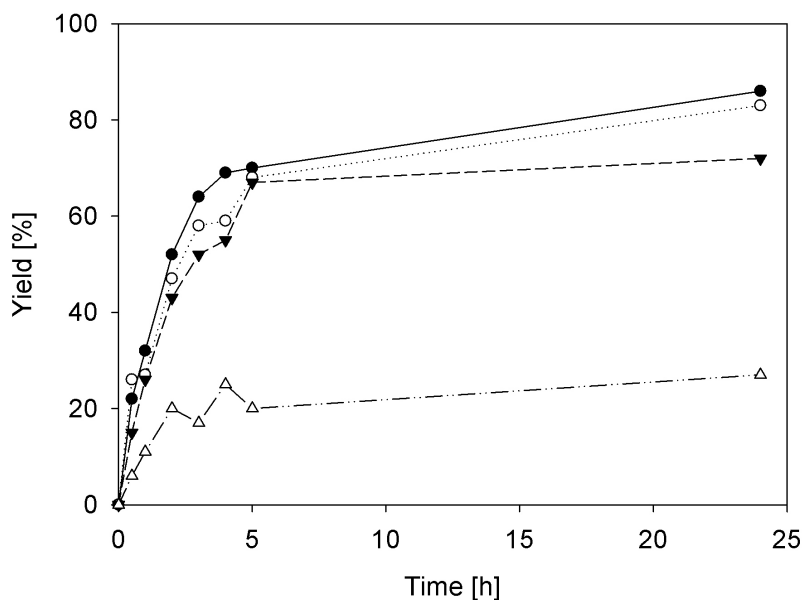


Figure 2. Time courses of resin-based whole cell bioreductions varying substrate and resin concentrations. Conditions: *E. coli* BL21 (DE3) pETDuet1_XR_FDHD (whole cells); [cells] = 40 g_{CDW}/L; pH 7.5; 30°C; 30 rpm. Symbols: ● = 100 mM *o*-chloroacetophenone + 30 vol% resin; ○ = 100 mM *o*-chloroacetophenone + 40 vol% resin; ▼ = 100 mM *o*-chloroacetophenone + 35 vol% resin; Δ = 200 mM *o*-chloroacetophenone + 60 vol% resin.

Intracellular cofactor availability and mass transfer over the membrane are two central problems in whole cell biocatalysis. The passive uptake of hydrophobic compounds occurs by simple diffusion into the cellular membrane whereas polar or charged molecules can not enter the cell without importer.^[14] Addition of 500 μM NAD^+ to resin-based *E. coli* whole cell bioreductions did neither increase yield nor product formation rate indicating that the presence of a low organic substrate concentration and the resin does not permeabilize *E. coli* cells (Figure 3). We and others have previously shown that the yields of bioreductions can be enhanced by making the cell wall more easily permeable for external NAD^+ , substrates and products.^[8,15-20] The antibiotic polymyxin B sulphate shows a locally disruptive effect on cell wall integrity of gram-negative bacteria^[21] by binding to the lipid A portion of bacterial lipopolysaccharides and induction of pore formation in the membrane.^[22]

However, simultaneous addition of polymyxin B sulphate and NAD^+ did not increase product yield suggesting deactivation of polymyxin B sulphate by absorption onto the polymeric adsorbent.

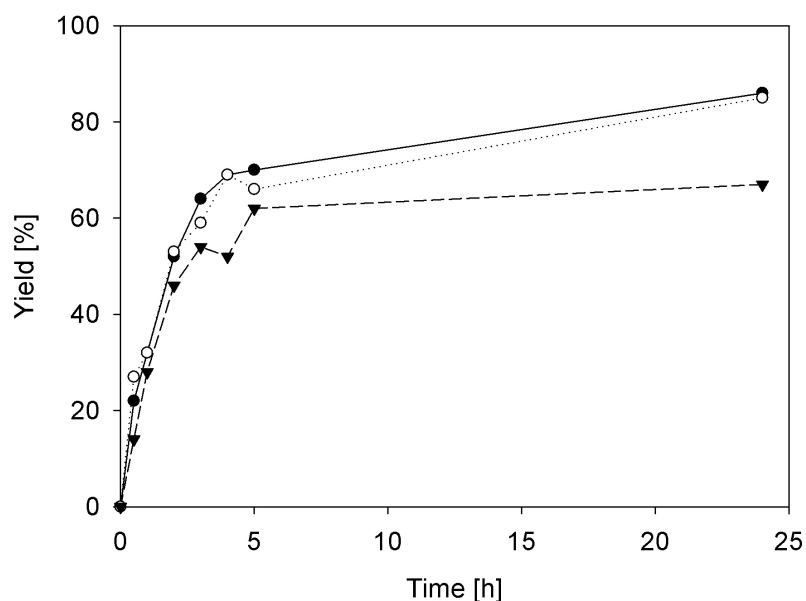


Figure 3. Effects of externally added NAD^+ and cell permeabilization on resin-based, whole cell bioreductions of *o*-chloroacetophenone. Conditions: *E. coli* BL21 (DE3) pETDuet1_XR_FDHD (whole cells); [cells] = 40 g_{CDW}/L; [substrate] = 100 mM; pH 7.5; 30°C; 30 rpm. Symbols: ● = + 30 vol% resin; ○ = + 30 vol% resin + NAD^+ [500 μM]; ▼ = + 30 vol% resin + NAD^+ [500 μM] + polymyxin B sulphate [36 μM].

2.3.2. ISSS and ISPR by Organic Co-solvents

Water-immiscible organic co-solvents act as substrate reservoir and *in situ* product extracting agents in biocatalysis of toxic, hydrophobic compounds. The *n*-octanol-water partition coefficient ($\log P$) of organic solvents correlates to cell-toxicity of the second organic phase given that transfer of hydrophobic substrates and products proceeds via dissolution in the aqueous phase and subsequent (passive) uptake by the cell. Hydrophobic compounds accumulate in the cell membrane, thereby effecting permeabilization and cell integrity.^[14,23-25] Direct contacts between solid or liquid second phases are of less toxicity to the cells.^[26] We

have previously shown that organic solvents with $\log P < 2$ are not suitable for biocatalytic systems.^[8,9] Water immiscible ionic liquids have been described as biocompatible and not damaging to cells in whole cell bioreductions.^[27,28] We therefore chose highly hydrophobic dodecane ($\log P$ 6.8), heptane ($\log P$ 4.66) and hexane ($\log P$ 4.11) and one ionic liquid (1-butyl-3-methylimidazolium hexafluorophosphate (BMIMPF₆)) as most promising second phases. Results of two-phasic whole cell reductions of 100 mM *o*-chloroacetophenone are shown in Figure 4. The product (*S*)-1-(2-chlorophenyl)ethanol was obtained in 84 % yield with 20 % (v/v) hexane compared to 66 % with heptane, 27 % with dodecane and 31 % with the ionic liquid and 16 % lacking a second phase. Similar experiments with 50 % (v/v) co-solvents resulted in significantly lower yields. Thus, differences in yield are mainly due to the effective substrate concentration in the aqueous phase and the toxicity and interfacial area of the second phase. Very low substrate concentrations in the aqueous phase decrease the intracellular substrate availability by slowing down the enzymatic reaction given that enzymatic rate is linearly dependent on substrate concentration ($K_{o\text{-chloroacetophenone}} > 5$ mM).

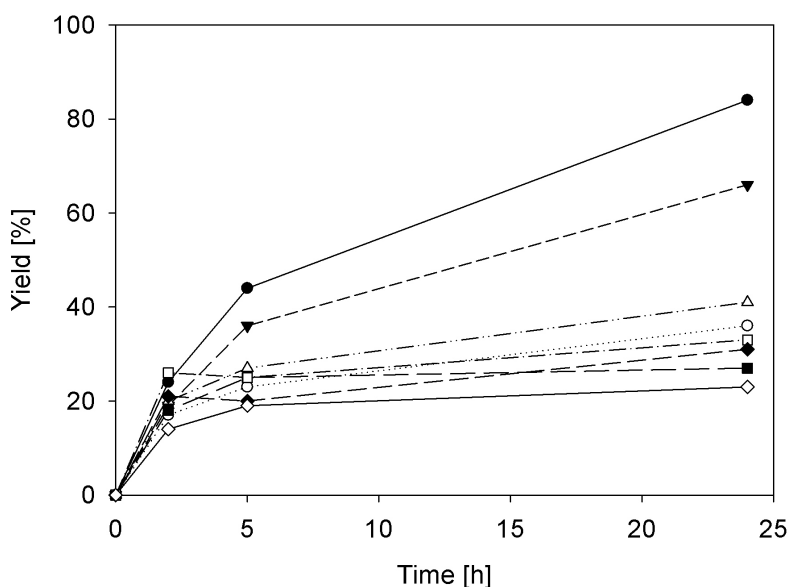


Figure 4. Effects of co-solvent amount and type on whole cell bioreduction rates of *o*-chloroacetophenone. Conditions: *E. coli* BL21 (DE3) pETDuet1_XR_FDHD (whole cells); [cells] = 40 g_{CDW}/L; [substrate] = 100 mM; pH 7.5; 30°C; 30 rpm. Symbols: ● = + 20 vol% hexane; ○ = + 50 vol% hexane; ▼ = + 20 vol% heptane; △ = + 50 vol% heptane; ■ = + 20 vol% dodecane; □ = + 50 vol% dodecane; ◆ = + 20 vol% BMIMPF₆; ◇ = + 50 vol% BMIMPF₆.

Figure 5 shows the effects of NAD⁺ and polymyxin B sulphate addition on yields and reaction rates in two-phasic reductions. NAD⁺ supplementation without antibiotic cell permeabilization enhanced reduction yields in reactions with hexane and heptane as second phase. Further permeabilization with polymyxin B sulphate resulted in complete conversion (analytical yield of 98 %). No improvement by addition of external NAD⁺ and polymyxin B sulphate was observed in two phasic reactions with dodecane and BMIMPF₆ indicating a low substrate concentration and deactivation of polymyxin B sulphate.

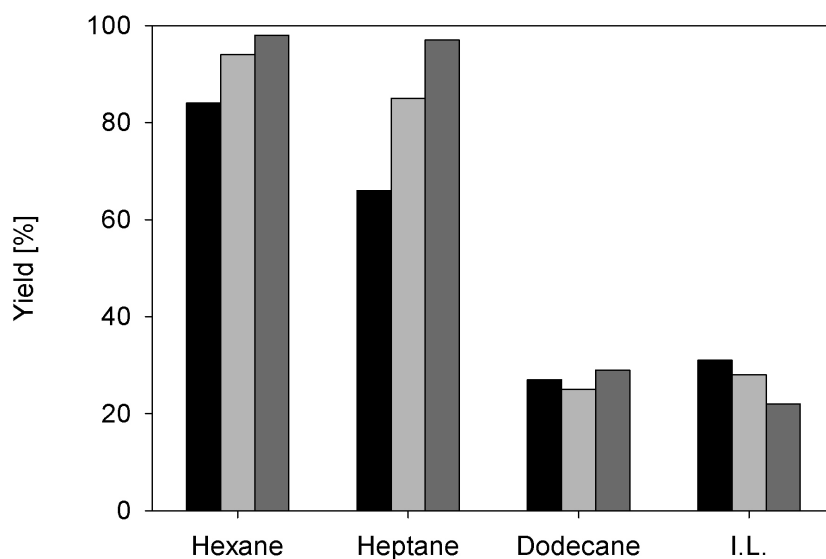


Figure 5. Optimization of 100 mM *o*-chloroacetophenone reduction by *E. coli* BL21 (DE3) pETDuet1_XR_FDHD (whole cells). The effects of organic co-solvents, cell permeabilization and externally added NAD⁺ on yields. Conditions: [cells] = 40 g_{CDW}/L; [substrate] = 100 mM; [co-solvents] = 20 vol%; reaction time 24 h; pH 7.5; 30°C; 30 rpm. Black bars: experiment with co-solvent; Grey bars: with additional NAD⁺ [0.5 mM]; Dark grey bars: with additional NAD⁺ [500 µM] and polymyxin B sulphate [36 µM]. I.L. = ionic liquid (BMIMPF₆).

Encouraged by the complete conversion of 100 mM *o*-chloroacetophenone in the hexane/water system supplemented with NAD⁺ and polymyxin B sulphate we performed asymmetric reduction of 200 mM *o*-chloroacetophenone. Figure 6 shows the results of whole cell catalyzed reductions of 200 mM *o*-chloroacetophenone with 20 % (v/v), 30 % (v/v) and 40 % (v/v) hexane. Again highest conversions were obtained with 20 % hexane suggesting the interfacial area to more seriously effect cell stability than substrate concentration. Supplementation with NAD⁺ and polymyxin B sulphate increased conversion from 120 to 164 mM as compared to the non supplemented reaction. Addition of hexane, NAD⁺ and polymyxin B sulphate increased the yield 12-fold as compared to the reaction in plain buffer.

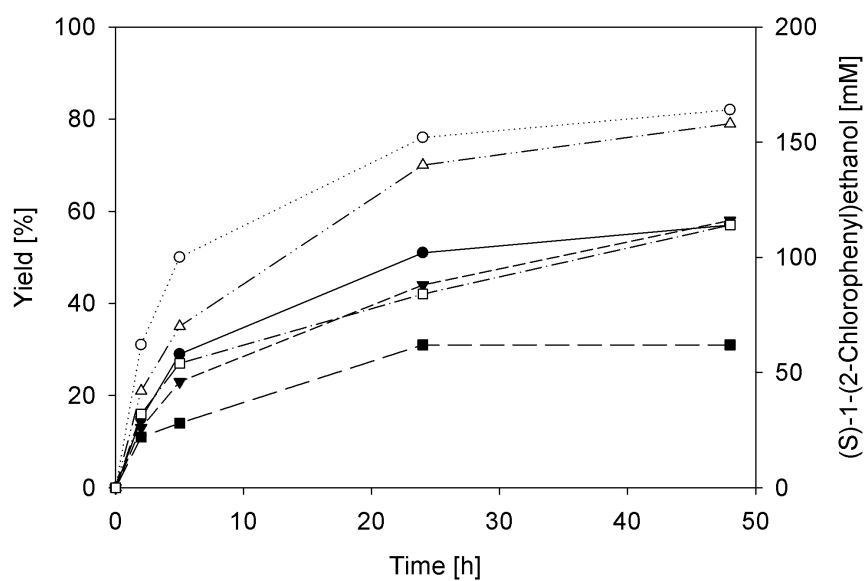


Figure 6. Optimization of the 200 mM *o*-chloroacetophenone reduction. The effects of different co-solvent concentrations on yields. Conditions: *E. coli* BL21 (DE3) pETDuet1_XR_FDHD (whole cells); [cells] = 40 g_{CDW}/L; [substrate] = 200 mM; pH 7.5; 30°C; 30 rpm. Symbols: ● = + 20 vol% hexane; ○ = + 20 vol% hexane + NAD⁺ (500μM) + PM (50mg/L); ▼ = + 30 vol% hexane; Δ = + 30 vol% hexane + NAD⁺ (500μM) + PM (50mg/L); ■ = + 40 vol% hexane; □ = + 40 vol% hexane + NAD⁺ (500μM) + PM (50mg/L).

2.4. Effect of Different *E. coli* Strains

The specific activities of isolated CtXR (determined with *o*-chloroacetophenone) and CbFDH compare roughly to 4.4 U/mg.^[29] We used pETDuet-1b designed for simultaneous expression of two genes to co-express CtXR and CbFDH in *E. coli* BL21 (DE3). However the activity ratio of CtXR/CbFDH in *E. coli* BL21 (DE3) pETDuet1_XR_FDHDH was determined to 11, suggesting a kinetic bottleneck in the recycling of NADH during whole cell reduction of *o*-chloroacetophenone.^[8,9] We therefore increased the intracellular CbFDH expression by an additional plasmid carrying the FDH gene (pRSF) and expression in *E. coli* Rosetta2 (termed *E. coli* Rosetta2 pETDuet1_XR_FDHDH + pRSF_FDHDH). We compared both strains in whole cell reductions of 100 mM substrate with 30 % (v/v) resin AMBERLITE™ XAD7HP and 200 mM substrate with 20 % hexane as second phases. Experiments with resin showed no detectable difference between the two strains (data not shown) indicating again mass transfer and substrate availability as main obstacle in resin-based bioreductions. Conversion of 200 mM substrate in 20 % hexane supplemented with NAD⁺ and polymyxin B sulphate yielded 76 % product with both strains, the initial reduction rate, however, was doubled with *E. coli* Rosetta2 pETDuet1_XR_FDHDH + pRSF_FDHDH (Figure 7). We therefore used the Rosetta 2 strain in all further experiments.

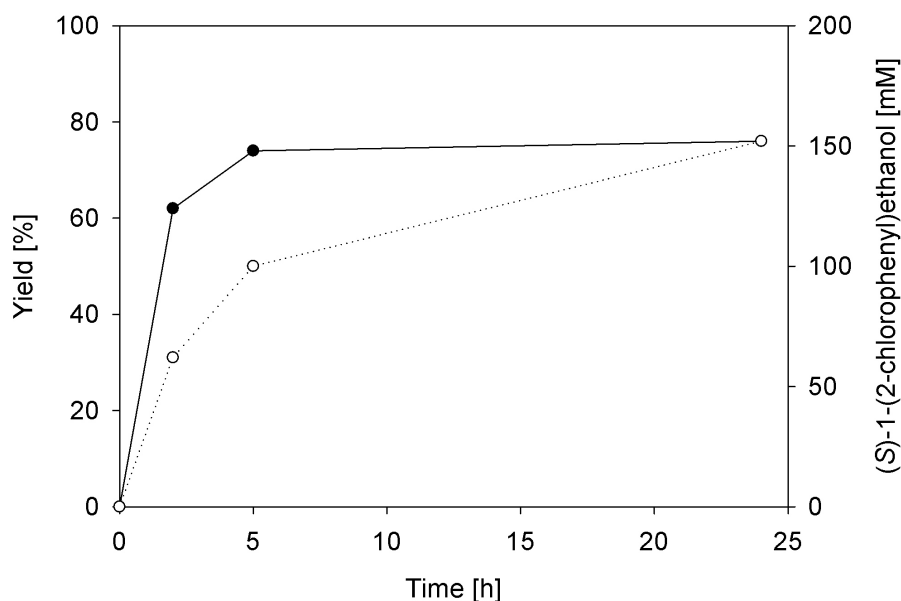


Figure 7. Comparison of *o*-chloroacetophenone reduction with two different whole-cell catalysts. Conditions: [cells] = 40 g_{CDW}/L; [substrate] = 200 mM; [hexane] = 20 % (v/v); [NAD⁺] = 500 μM; [polymyxin B sulphate] = 36 μM; pH 7.5; 30°C; 30 rpm. Symbols: ● = *E. coli* Rosetta2 pETDuet1_XR_FDHD + pRSF_FDHD; ○ = *E. coli* BL21 (DE3) pETDuet1_XR_FDHD.

2.5. Effect of pH

E. coli whole cell reductions are generally performed at pH values of 6.5 or 7.0 and, to the best of our knowledge, no pH optimization has been performed to date.^[30,38,39,41] We therefore compared four different pH values between 7.5 and 6.2 to improve (S)-1-(2-chlorophenyl)ethanol production and to study the effect of pH on *o*-chloroacetophenone reduction. The isolated CbFDH shows no pH-dependence in the indicated interval whereas the specific activity of CtXR determined with xylose more than doubled in response to a decrease in pH from 7.5 to 6.2 (see Figure 8). Yields in batch conversions of 100 mM or 200 mM *o*-chloroacetophenone reflected the pH dependence of CtXR at pH 7.5, 7.0, 6.5 and 6.2

(Figure 8). A pH change from 7.5 to 6.2 caused a two-fold yield increase in batch conversions of 100 mM and 200 mM *o*-chloroacetophenone. We determined analytical yields of 63 % with 100 mM substrate and 31 % with 200 mM substrate. Higher conversions at lower pH values can be explained by higher XR activities suggesting a high perforation level of the cell and hence equal inter- and intracellular pH values. However, assuming limiting NADH-recycling, an increase in XR-activity alone might not lead to higher conversions. Formate is an ideal co-substrate for the regeneration of NADH since oxidation is thermodynamically favoured, and the co-product carbon dioxide is easily removed from the reaction mixture.^[27,30-35] Thus, for a successful bioreduction of *o*-chloroacetophenone a fast formate import into the cell is required. Passive transport of formate in the undissociated, membrane-permeable form might be of minor importance at pH-values between 6.2 and 7.5, taking a formate pK_a of 3.75 into account. So far, one protein involved in formate transport in and out of the anaerobic cell, namely FocA (formate channel), has been identified. The membrane protein encoded by *focA* regulates the anaerobic formate pool in pH dependence. Once the extracellular pH drops below 6.8, formate is rapidly and completely imported into the cells.^[36,37] The influence of buffer pH to formate import remains speculative taking a high perforation level of the cell into account. Especially if considering that the use of different pH values did not make an impact on yields in resin-based experiments i.e. non-perforating conditions (data shown in appendix chapter B.3.1.).

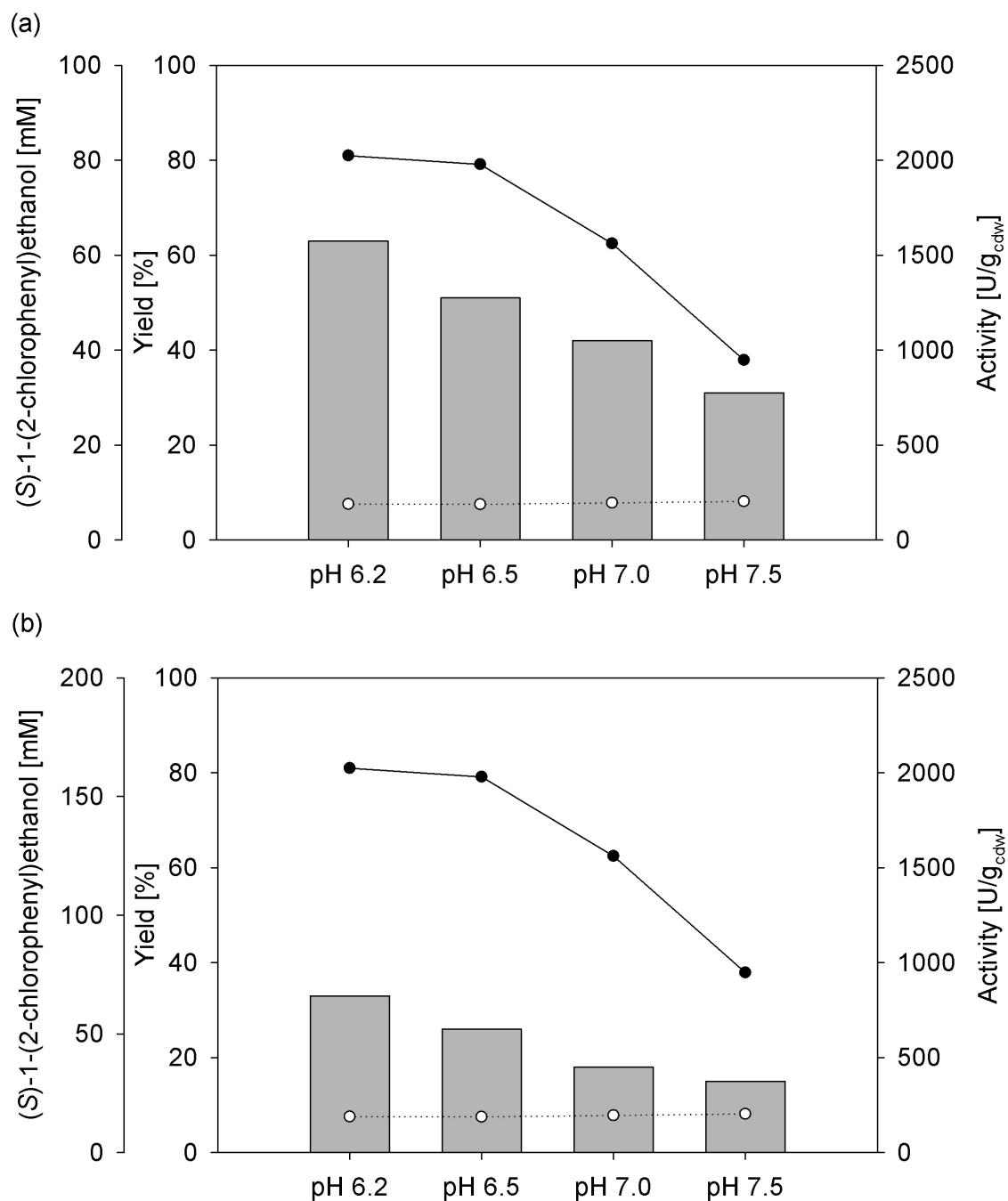


Figure 8. Effect of different pH-values on XR- and FDH-activity and corresponding chemical yields. Reaction conditions: *E. coli* Rosetta2 pETDuet1_XR_FDH + pRSF_FDH; Conversion: [cells] = 40 g_{CDW}/L; 30°C; 30 rpm; 24 h. (a) [substrate] = 100 mM, (b) [substrate] = 200 mM. Enzyme-activity: crude cell extract, [xylose] = 700 mM; [sodium formate] = 200 mM; reaction time = 5 min; 25°C; ● = XR; ○ = FDH.

Under perforating conditions i.e. in a two-phasic system using 20 % hexane supplemented with NAD^+ and polymyxin B sulphate, a decrease in pH from 7.5 to 6.2 led to complete conversion (98 %) and 1.5-fold increase in yield. An analytical yield of 95 % corresponding to 285 mM was determined in a similar experiment using equal parameters but 300 mM substrate. The resulting *o*-chloroacetophenone reduction rate (r_s) of $\sim 93 \text{ U/g}_{\text{CDW}}$, expected from the corresponding enzyme activity (CbFDH in *E. coli* Rosetta2 pETDuet1_XR_FDH + pRSF_FDH), obtained from measurement of product formation after 30 min, indicate that mass transfer is not longer limiting, when using a biphasic system with 20 % hexane supplemented with NAD^+ and polymyxin B sulphate.

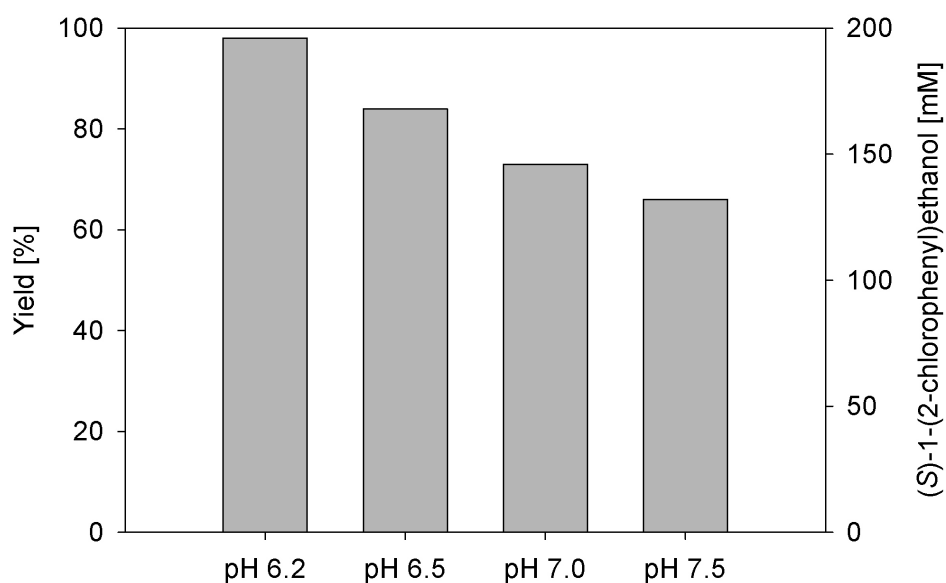


Figure 9. Chemical yield under different pH values in hexane/water system. Conditions: *E. coli* Rosetta2 pETDuet1_XR_FDH + pRSF_FDH; [cells] = 40 $\text{g}_{\text{CDW}}/\text{L}$; [substrate] = 200 mM; [hexane] = 20 % (v/v); 30°C; 30 rpm; 24 h.

2.6. Scale-up and Downstream-processing

We performed whole cell bioreduction on a 15 mL-scale to demonstrate scalability of resin-based and two-phasic whole cell bioreductions. Workup issues are often neglected in whole cell biocatalysis and hardly found in literature even though they have a huge impact on the isolated yield.^[38,39,42] We therefore tried to simplify product isolation of resin-based and two-phasic whole cell bioreductions as schematically depicted in Figure 10. The analytical yield after bioreduction of 100 mM *o*-chloroacetophenone with 30 % (v/v) resin was determined to 91 %. The product (*S*)-1-(2-chlorophenyl)ethanol was two-fold extracted with ethyl acetate yielding 76 and 21 %. No product and no substrate could be found in the aqueous phase, indicating 5 % of the product lost in the biomass. The product solution was dried with concomitant loss of 6 % product prior to ethyl acetate evaporation at reduced pressure. The product (*S*)-1-(2-chlorophenyl)ethanol was isolated in a preparative yield of 91 % (0.21 g) as colourless liquid. An analytical yield of 97 % was obtained in two-phasic bioreductions using 300 mM substrate, 20 % (v/v) hexane supplemented with NAD⁺ and polymyxin B sulphate. The overall yield after three extraction-steps (no product lost in the aqueous phase) was 88 % (*S*)-1-(2-chlorophenyl)ethanol. We omitted drying of the hexane phase due to low water solubility in hexane. An isolated yield of 88 % (0.62 g) was determined after hexane evaporation at reduced pressure. The two-phasic bioreduction using 20 % hexane seems not only preferable due to higher conversions but also regarding downstream processing. Use of the same organic solvent as co-solvent in bi-phasic reactions and as extraction media reduces process complexity and number of steps.

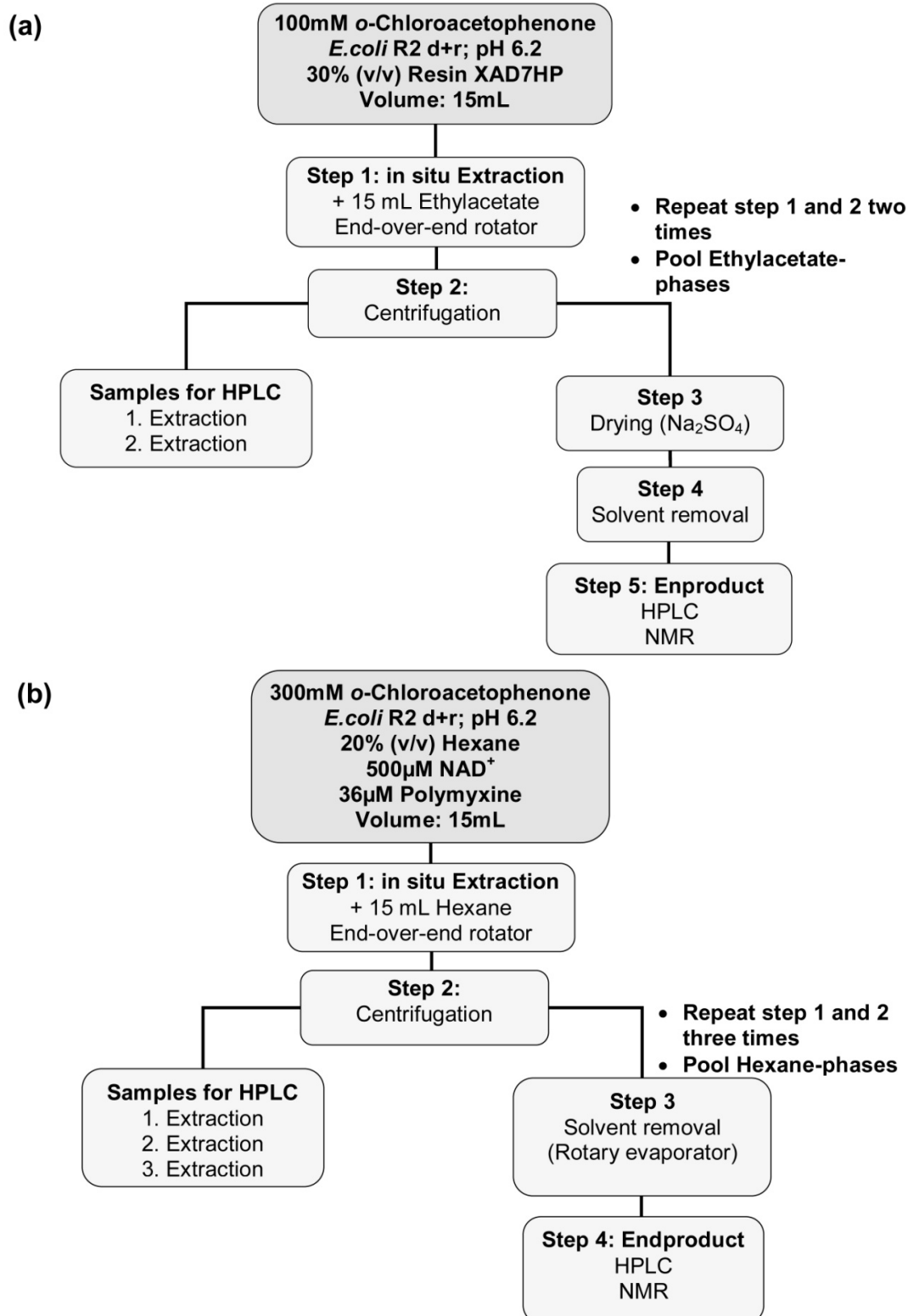


Figure 10. Setup for the scale-up experiments with (a) resin or (b) hexane and the schematic view of the downstream-processing. Conditions: *E. coli* Rosetta2 pETDuet1_XR_FDHD + pRSF_FDHD (whole cells); [cells] = 40 g_{CDW}/L; Reaction time = 24 h.

3. Conclusions

Substrate toxicity toward biocatalysts is an often observed problem that can undermine otherwise good processes. The investigations carried out in this paper to uncover the reasons behind the short biocatalyst half-life and the methods to (at least partially) overcome the problems will be a useful guide to other workers in the field.

CtXR is a rare and powerful catalyst for the reduction of *o*-chloroacetophenone in absolute optical purity. This paper provides how whole cell-based biocatalytic reaction of this poorly soluble and toxic substrate can be greatly enhanced by ISSS and ISPR with polymeric adsorbent resins and different organic co-solvents. Most successful was the use of 20 % (v/v) hexane, NAD⁺ and polymyxin B sulphate resulting in an enhanced product concentration of 285 mM (yield: 95 %). Unfortunately, utilization of the resin, which overcomes the disadvantages of traditional organic solvents (poor biocompatibility, volatilization and environmentally harmful), was limited to 100 mM substrate because of stirring problems. Application of fed-batch processes showed only little enhancement in the obtained yield which was due to inhibition or toxicity of the substrate and product to the whole cells.

4. Experimental Section

4.1. Chemicals, Materials and Strains

Racemic 1-(2-chlorophenyl)ethanol was from Alfa Aesar GmbH & Co KG (Karlsruhe, Germany). NADH (sodium salt; $\geq 98\%$ pure) and NAD⁺ (free acid; $\geq 97.5\%$ pure) were obtained from Roth (Karlsruhe, Germany). The resin AmberliteTM XAD7HP (free of charge sample) was from Rohm and Haas (Coventry, U.K.). The ionic liquid 1-butyl-3-methylimidazolium hexafluorophosphate (BMIMPF₆; product number 18122) was from Sigma-Aldrich (Vienna, Austria). All other chemicals were purchased from Sigma-Aldrich / Fluka (Gillingham, Dorset, U.K.) or Roth (Karlsruhe, Germany), and were of the highest purity available. 15 mL tubes were purchased at Sarstedt (Wr. Neudorf, Austria). 2 mL Eppendorf tubes were purchased at Eppendorf Austria GmbH (Wien, Austria).

The microorganisms used were *E. coli* BL21 (DE3) pETDuet1_XR_FDHD and *E. coli* Rosetta2 pETDuet1_XR_FDHD + pRSF_FDHD. *E. coli* BL21 (DE3) pETDuet1_XR_FDHD is the parent BL21 (DE3) strain harbouring the plasmid vector pETDuet-1 that is used for co-expression of the genes encoding CtXR and CbFDH (pETDuet_XR_FDHD).^[8] *E. coli* Rosetta2 pETDuet1_XR_FDHD + pRSF_FDHD is a Rosetta 2 strain containing pETDuet_XR_FDHD and an additional pRSF plasmid that encodes CbFDH (Master Thesis Katharina Mädje).

4.2. Cultivation of Strains

E. coli strains were grown in 1000 mL baffled shaken flasks containing 200 mL of LB media supplemented with 115 mg/L ampicillin. A Certomat® BS-1 incubator from Sartorius was used at a constant agitation rate of 120 rpm. Recombinant protein production used a standard procedure in which cultures were cooled from 37 °C to 18 °C when an optical density of 1.1 ($\pm 10\%$) was reached. Isopropylthio- β -D-galactoside (IPTG) was added in a concentration of 1.0 mM, and the cultivation time after induction was 20 h. Cells were harvested by centrifugation and broken up with the lysis reagent B-Per (Pierce, Rockford, IL, USA).

4.3. Enzyme Activity Measurements in the Cell-free Extracts

Reductase and dehydrogenase activities were assayed spectrophotometrically at 25 °C, monitoring the reduction or oxidation of NAD(H) at 340 nm over a time of 5 min. Typically, rates of 0.05 – 0.10 $\Delta A/\text{min}$ were measured. One unit of enzyme activity refers to 1 μmol of NAD(H) consumed per minute. All measurements were performed with a Beckman DU-800 spectrophotometer using 100 mM potassium phosphate buffer (pH 7.5, 7.0, 6.5, 6.2). The standard assay for *CtXR* contained 700 mM xylose and 300 μM NADH; that for *CbFDH* contained 200 mM sodium formate and 2 mM NAD^+ . Reactions were always started by the addition of coenzyme. Measured rates were corrected for appropriate blank readings accounting for non-specific oxidation or reduction of NAD(H) by the cell extracts.

4.4. Evaluation of Substrate and Product “Toxicity”

Reaction mixtures (10 mL) containing 40 g_{CDW}/L *E. coli* BL21 (DE3) pETDuet1_XR_FDHD and different concentrations between 0 and 50 mM *o*-chloroacetophenone or (*S*)-1-(2-chlorophenyl)ethanol in 100 mM potassium phosphate buffer, pH 7.5, were incubated in 15 mL Sarstedt tubes at 30 °C. The mixing was done with an end-over-end rotator (SB3 from Stuart) at 30 rpm. Samples (100 µL) were taken after 0.25, 0.5, 1, 1.5, 2, 3, 4 and 5 h. The reaction mixture was diluted 20-fold with buffer such that no organic phase (from insoluble substrate) remained, and cells were then collected by centrifugation. After cell lysis using B-Per, enzyme activities were assayed as described above.

4.5. Whole-cell Bioreduction of *o*-Chloroacetophenone

Experiments were carried out at 30 (± 1) °C using 2-mL Eppendorf reaction tubes (batch experiments) or 15-mL Sarstedt tubes (fed-batch experiments) that were incubated in an end-over-end rotator (SB3 from Stuart) at 30 rpm. *E. coli* cells in a concentration between 30 and 80 g_{CDW}/L were suspended in 100 mM potassium phosphate buffer (pH 7.5, 7.0, 6.5, 6.2). *o*-chloroacetophenone is a liquid and was added in a concentration between 3 and 300 mM as indicated. The substrate was dissolved in ethanol to give a final ethanol concentration of maximally 5 % (by weight). It was shown in earlier work that this level of ethanol does not interfere with CtXR activity and stability.^[40] Because the solubility of *o*-chloroacetophenone was only 10 mM under the conditions used, reactions with substrate concentrations of > 10 mM, took place in an aqueous-organic two-phase system (micro emulsion). The concentration

of sodium formate always exceeded that of the ketone substrate by 50 mM (minimum 80 mM). The total reaction volume was 1 mL (batch) or 10 mL (fed batch), and conversions were started through addition of substrate. For different substrate feed rates in fed-batch processes see Table 1.

In resin-based conversions, the polymeric absorbent AMBERLITE™ XAD7HP was washed with distilled water and 100 mM potassium phosphate buffer, pH 6.2 prior to substrate loading. Presorption of substrate was accomplished by gently mixing the substrate and the washed resin in buffer (0.5 mL total volume) on an end-over-end rotator for 2 h at 30 °C and 30 rpm. The reaction was started by addition of 0.5 mL *E. coli* cell-suspension (80 g_{CDW}L⁻¹) and co-substrate. After specified reaction times product and unconverted substrate were desorbed with ethanol (1:1 ratio) at 50 °C for 2 h (950 rpm).

In reactions where a water-immiscible organic co-solvent (hexane, heptane, dodecane) or ionic liquid (BMIMPF₆) was used, the substrate was dissolved in the co-solvent (20 % v/v to 50 % v/v) first and added to the aqueous phase containing the cells. 1 mL samples were taken at certain times, typically every hour, and analyzed as described under Analytical Methods.

Preparative synthesis of (*S*)-1-(2-chlorophenyl)ethanol with 20 % v/v hexane as co-solvent was performed in a total volume of 15 mL. 0.6 g_{CDW} of *E. coli* Rosetta2 pETDuet1_XR_FDHD + pRSF_FDHD and 5.25 mmol sodium formate was diluted into 12 mL 100 mM potassium phosphate buffer pH 6.2, supplemented with 500 μM NAD⁺ and 36 μM polymyxin B sulphate. The reaction was started by addition of 4.5 mmol *o*-chloroacetophenone in 3 mL hexane. After 24 h incubation in situ extraction of product and remaining substrate was performed by hexane addition in a 1:1 ratio using three times 15 mL and incubation in an end-over-end rotator (SB3 from Stuart) at 30 rpm (room temperature) for 2 h. After centrifugation

at 5000 g for 20 min the withdrawn organic phases were united, and hexane was evaporated under reduced pressure.

Preparative synthesis of (*S*)-1-(2-chlorophenyl)ethanol with 30 % v/v polymeric adsorbent AMBERLITE™ XAD7HP was performed in a total volume of 15 mL. The reaction mixture contained 0.6 g_{CDW} of *E. coli* Rosetta2 pETDuet1_XR_FDH + pRSF_FDH, 1.5 mmol *o*-chloroacetophenone, 30 % v/v resin and 2.25 mmol sodium formate in a 100 mM potassium phosphate buffer, pH 6.2. After 24 h incubation in situ extraction of product and remaining substrate was performed by ethyl acetate addition in a 1:1 ratio using two times 15 mL and incubation in an end-over-end rotator (SB3 from Stuart) at 30 rpm (30 °C) for 1 h. After centrifugation at 5000 g for 20 min the withdrawn organic phases were united, dried with sodium sulphate, and ethyl acetate was evaporated under reduced pressure.

4.6. Analytical Methods

All samples not containing a second liquid phase were diluted with ethanol as required to obtain a homogeneous liquid phase. Biomass was separated by centrifugation prior to dilution of supernatants and organic-phases into the mobile phase (20 % v/v acetonitrile) to concentrations of < 50 mM analyte. Chiral HPLC was performed on a LaChrom HPLC system (Merck-Hitachi) equipped with a reversed phase CHIRALPAK AD-RH column from Daicel (purchased at VWR International, Vienna, Austria) and an L-7400 UV-detector. Detection was at 210 nm.^[40] Baseline separation of the *R* and *S* antipode in a racemic mixture of 1-(2-chlorophenyl)ethanols was obtained when using 20 % v/v acetonitrile as eluent at a flow rate of 0.5 mL/min and a temperature of 40 °C. Authentic standards were used for peak

identification, and quantification was based on peak area that was suitably calibrated with standards of known concentration. The detection limits of *o*-chloroacetophenone and 1-(*o*-chlorophenyl)-ethanols were below 0.005 mM. Reported yields of product on substrate consumed are always from analytical data except of the determination of the overall yield in the scale-up experiments.

5. References

- [1] A. Santamaria, R. Neef, U. Eberspächer, K. Eis, M. Husemann, D. Mumberg, S. Prechtel, V. Schulze, G. Siemeister, L. Wortmann, F. A. Barr, E. A. Nigg, *Mol. Biol. Cell.* **2007**, *18*, 4024-4036.
- [2] Y. Sato, Y. Onozaki, T. Sugimoto, H. Kurihara, K. Kamijo, C. Kadowaki, T. Tsujino, A. Watanabe, S. Otsuki, M. Mitsuya, M. Iida, K. Haze, T. Machida, Y. Nakatsuru, H. Komatani, H. Kotani, Y. Iwasawa, *Bioorg. Med. Chem. Lett.* **2009**, *19*, 4673-4678.
- [3] T. R. Rheault, M. Cheung, J. G. B. Alberti, K. H. Donaldson, *PCT Int. Appl.* **2008**, WO 2008070354 A2 20080612.
- [4] T. Stengel, M. Schmidt, S. Weinbrenner, A. Weber, P. Gimmnich, V. Gekeler, T. Beckers, A. Zimmermann, T. Maier, B. Schmidt, F. Dehmel, *PCT Int. Appl.* **2009**, WO 2009003911 A1 20090108.
- [5] W. Baratta, M. Ballico, S. Baldino, G. Chelucci, E. Herdtweck, K. Siega, S. Magnolia, P. Rigo, *Chem. A. Eur. J.* **2008**, *14*, 9148-9160.
- [6] D. A. Evans, F. E. Michael, J. S. Tedrow, K. R. Campos, *J. Am. Chem. Soc.* **2003**, *125*, 3534-3543.
- [7] S. Zeror, J. Collin, J. C. Fiaud, L. A. Zouioueche, *Adv. Synth. Catal.* **2008**, *350*, 197-204.
- [8] R. Kratzer, M. Pukl, S. Egger, B. Nidetzky, *Microb. Cell Fact.* **2008**, *7*, 37-48.
- [9] R. Kratzer, M. Pukl, S. Egger, M. Vogl, L. Brecker, B. Nidetzky, *Biotechnol. Bioeng.* **2010**, in press.
- [10] P.-Y. Kim, D. J. Pollard, J. M. Woodley, *Biotechnol. Prog.* **2007**, *23*, 74-82.

- [11] J. T. Vicenzi, M. J. Zmijewski, M. R. Reinhard, B. E. Landen, W. L. Muth, P. G. Marler, *Enzyme Microb. Tech.* **1997**, *20*, 494-499.
- [12] J.-L. Guo, X.-Q. Mu, Y. Xu, *Bioprocess Biosyst. Eng.* **2009**, Epub ahead of print.
- [13] Rohm and Haas.
http://www.dow.com/assets/attachments/business/process_chemicals/amberlite_xad/amberlite_xad7_hp/tds/amberlite_xad7hp.pdf
- [14] J. Sikkema, J. A. M. de Bont, B. Poolman, *Microbiol. Rev.* **1995**, *59*, 201-222.
- [15] J. Zhang, B. Witholt, Z. Li, *Chem. Commun.* **2006**, *4*, 398-400.
- [16] M. Andersson, H. Holmberg, P. Adlercreutz, *Biotechnol. Bioeng.* **1998**, *57*, 79-86.
- [17] M. Andersson, R. Otto, H. Holmberg, P. Adlercreutz, *Biocatal. Biotransform.* **1997**, *15*, 281-296.
- [18] P. Adlercreutz, *Enzyme. Microb. Technol.* **1991**, *13*, 9-14.
- [19] H. Felix, P. Brodelius, K. Mosbach, *Anal. Biochem.* **1981**, *116*, 462-470.
- [20] A. Honorat-Pascal, F. Monot, D. Ballerini, *Appl. Microbiol. Biotechnol.* **1990**, *34*, 236-241.
- [21] M. Cánovas, T. Torroglosa, J. L. Iborra, *Enzyme Microb. Technol.* **2005**, *37*, 300-308.
- [22] H. Tsubery, I. Ofek, S. Cohen, M. Fridkin, *J. Med. Chem.* **2000**, *43*, 3085-92.
- [23] Z. Zahir, K. D. Seed, J. J. Dennis, *Extremophiles* **2006**, *10*, 129-138.
- [24] R. Aono, H. Kobayashi, *Appl. Environ. Microbiol.* **1997**, *63*, 3637-3642.
- [25] S. G. Griffin, S. G. Wyllie, J. L. Markham, D. N. Leach, *Flavour Frag. J.* **1999**, *14*, 322-332.
- [26] J. A. M. de Bont, *Trends Biotechnol.* **1998**, *16*, 493-499.
- [27] S. Bräutigam, S. Bringer-Meyer, D. Weuster-Botz, *Tetrahedron: Asymm.* **2007**, *18*, 1883-1887.

- [28] S. Bräutigam, D. Dennewald, M. Schürmann, J. Lutje-Spelberg, W. R. Pitner, D. Weuster-Botz, *Enzyme Microb. Technol.* **2009**, *45*, 310-316.
- [29] S. Krahulec, G. C. Armao, H. Weber, M. Klimacek, B. Nidetzky, *Carbohydr. Res.* **2008**, *343*, 1414-1423.
- [30] M. Ernst, B. Kaup, M. Müller, S. Bringer-Meyer, H. Sahm, *Appl. Microbiol. Biotechnol.* **2005**, *66*, 629-634.
- [31] B. Kaup, S. Bringer-Meyer, H. Sahm, *Appl. Microbiol. Biotechnol.* **2004**, *64*, 333-339.
- [32] A. Weckbecker, W. Hummel, *Biotechnol Lett* **2004**, *26*, 1739-1744.
- [33] H. Yamamoto, K. Mitsuhashi, N. Kimoto, Y. Kobayashi, N. Esaki, *Appl. Microbiol. Biotechnol.* **2005**, *67*, 33-39.
- [34] A. Menzel, H. Werner, J. Altenbuchner, H. Gröger, *Eng. Life Sci.* **2004**, *4*, 573-576.
- [35] H. Gröger, W. Hummel, C. Rollmann, F. Chamouleau, H. Hüsken, H. Werner, C. Wunderlich, K. Abokitse, K. Drauz, S. Buchholz, *Tetrahedron* **2004**, *60*, 633-640.
- [36] B. Suppmann, G. Sawers, *Mol. Microbiol.* **1994**, *11*, 965-982.
- [37] G. Sawers, *Biochem. Soc. Trans.* **2005**, *33*, 42-46.
- [38] H. Gröger, F. Chamouleau, N. Orogas, C. Rollmann, K. Drauz, W. Hummel, A. Weckbecker, O. May, *Angew. Chem. Int. Ed.* **2006**, *45*, 5677-5681.
- [39] T. Ema, O. Nobuyasu, I. Sayaka, T. Sakai, *Org. Biomol. Chem.* **2007**, *5*, 1175-1176.
- [40] R. Kratzer, B. Nidetzky, *Chem. Commun.* **2007**, *10*, 1047-1049.
- [41] N. Kizaki, Y. Yasohara, J. Hasegawa, M. Wada, M. Kataoka, S. Shimizu, *Appl. Microbiol. Biotechnol.* **2001**, *55*, 590-595.
- [42] R. Wohlgemuth, *J. Chem. Technol. Biotechnol.* **2007**, *82*, 1055-1062.

APPENDIX

A. Introduction

A.1. Polo-like Kinase 1 (PLK 1) Inhibitors

Thiophene-benzimidazoles and –imidazopyridines are among the most promising PLK1 inhibitor candidates. The modular assembly allows the systematic generation of inhibitor libraries by consecutive substitution of the thiophene, benzimidazole or imidazopyridine and phenylethanol groups.^[1,2,3] Chiral 1-(*o*-chlorophenyl)-ethanols turned out as chiral key intermediates in the synthesis of PLK1 inhibitors with good in vivo anti-tumor efficacy (Figure 11, red ellipse).^[1,4]

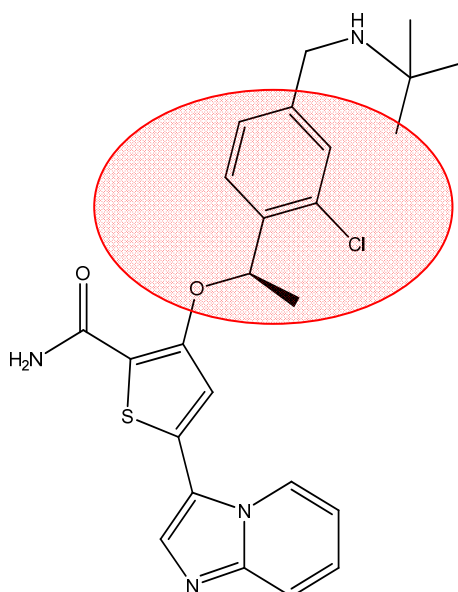


Figure 11. Imidazopyridine PLK1 inhibitor example with good anti-tumor efficacy.

B. Results and Discussion

B.1. Substrate and Product “Toxicity”

Half-life of enzymatic activity is the period of time it takes to decrease by half. We determined “rest-activities” of XR and FDH at different substrate- and product-concentrations over time. Activity loss followed an exponential decay in which activity decreases at a rate proportional to its value (equation 1). Integration leads to equation 2 respectively equation 3. Accordingly charts of the natural logarithm of rest-activity (fraction) versus time (min) were plotted. The half-life time was obtained from the slope following equation 4:

$$\frac{dEA}{dt} = -\lambda * EA \quad (1)$$

$$LN(EA_t) = -\lambda * t + C \quad (2)$$

$$EA_t = EA_0 * e^{-\lambda * t} \quad (3)$$

$$t_{1/2} = -\frac{LN(2)}{\lambda} \quad (4)$$

EA_t	enzyme activity at time t [U/g _{cdw}]
EA_0	enzyme activity at the beginning [U/g _{cdw}]
λ	decay constant [min ⁻¹]
t	time [min]
$t_{1/2}$	half-life [min]

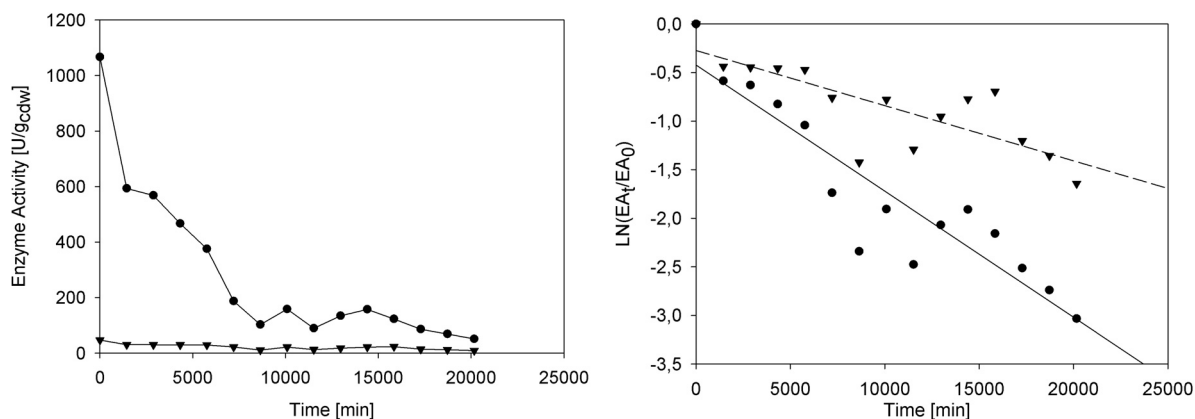


Figure 12. Half-life determination of XR- and FDH-activities in whole cell catalysts in the presence of 0 mM *o*-chloroacetophenone and 0 mM (*S*)-1-(2-chlorophenyl)ethanol. Conditions: *E. coli* BL21 (DE3) pETDuet1_XR_FDHD (whole cells); [cells] = 40 g_{CDW}/L; pH 7.5; 30°C; 30 rpm. Symbols: ● = XR, ▼ = FDH. XR-fit: $y = -0.0001x - 0.4229$; $R^2 = 0.8552$. FDH-fit: $y = -6E-05x - 0.2727$; $R^2 = 0.6375$.

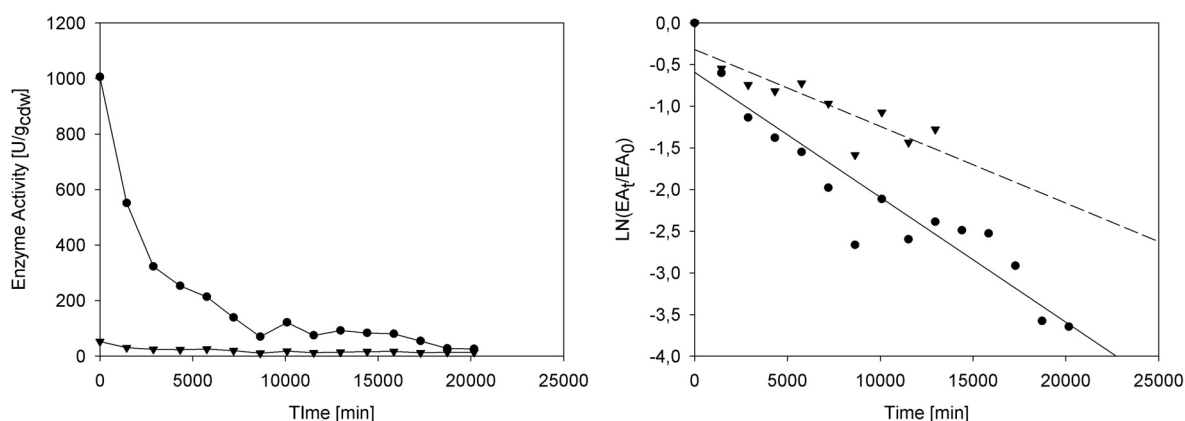


Figure 13. Half-life determination of XR- and FDH-activities in whole cell catalysts in the presence of 3 mM *o*-chloroacetophenone. Conditions: *E. coli* BL21 (DE3) pETDuet1_XR_FDHD (whole cells); [cells] = 40 g_{CDW}/L; pH 7.5; 30°C; 30 rpm. Symbols: ● = XR, ▼ = FDH. XR-fit: $y = -0.0001x - 0.5922$; $R^2 = 0.8909$. FDH-fit: $y = -9E-05x - 0.3193$; $R^2 = 0.755$.

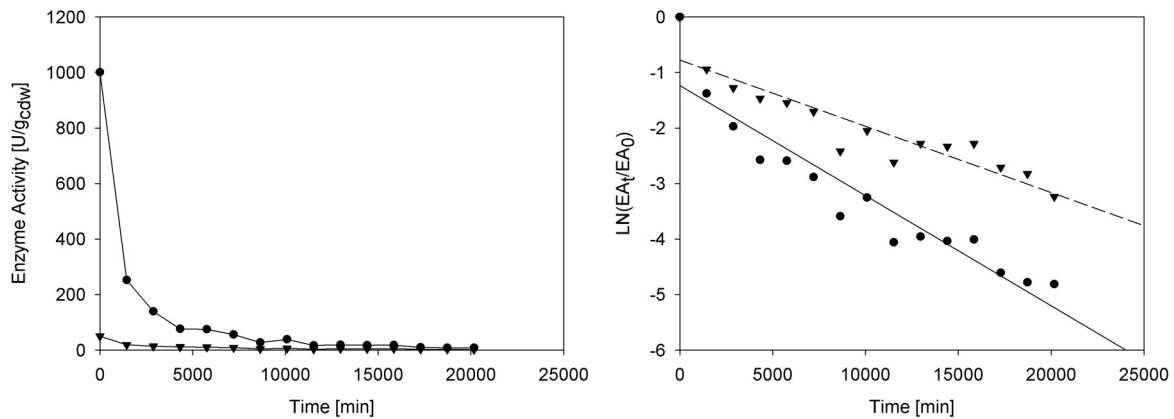


Figure 14. Half-life determination of XR- and FDH-activities in whole cell catalysts in the presence of 6 mM *o*-chloroacetophenone. Conditions: *E. coli* BL21 (DE3) pETDuet1_XR_FDH (whole cells); [cells] = 40 g_{CDW}/L; pH 7.5; 30°C; 30 rpm. Symbols: ● = XR, ▼ = FDH. XR-fit: $y = -0.0002x - 1.2336$; $R^2 = 0.8848$. FDH-fit: $y = -0.0001x - 0.7768$; $R^2 = 0.8467$.

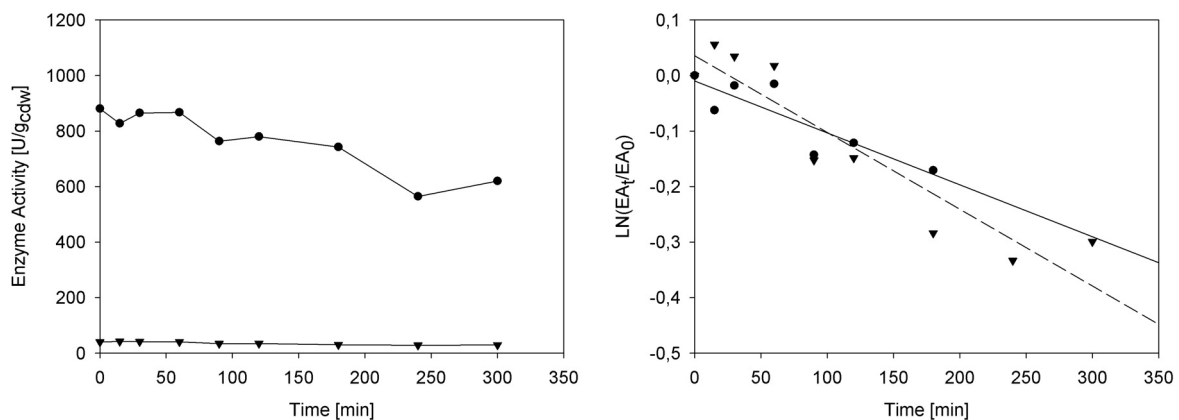


Figure 15. Half-life determination of XR- and FDH-activities in whole cell catalysts in the presence of 10 mM *o*-chloroacetophenone. Conditions: *E. coli* BL21 (DE3) pETDuet1_XR_FDH (whole cells); [cells] = 40 g_{CDW}/L; pH 7.5; 30°C; 30 rpm. Symbols: ● = XR, ▼ = FDH. XR-fit: $y = -0.0009x - 0.0098$; $R^2 = 0.7543$. FDH-fit: $y = -0.0014x + 0.0356$; $R^2 = 0.8665$.

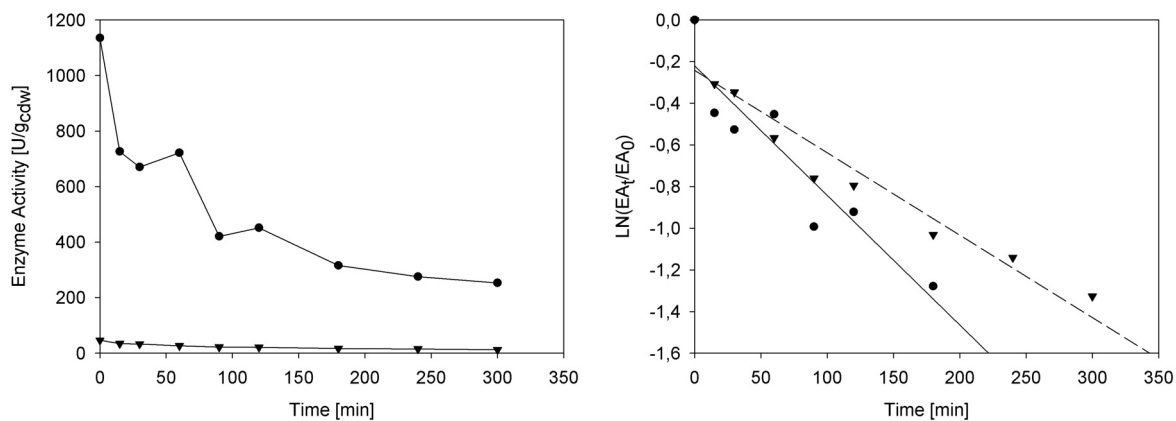


Figure 16. Half-life determination of XR- and FDH-activities in whole cell catalysts in the presence of 20 mM *o*-chloroacetophenone. Conditions: *E. coli* BL21 (DE3) pETDuet1_XR_FDHDH (whole cells); [cells] = 40 g_{CDW}/L; pH 7.5; 30°C; 30 rpm. Symbols: ● = XR, ▼ = FDH. XR-fit: $y = -0.0062x - 0.2202$; $R^2 = 0.8628$. FDH-fit: $y = -0.004x - 0.2424$; $R^2 = 0.9214$.

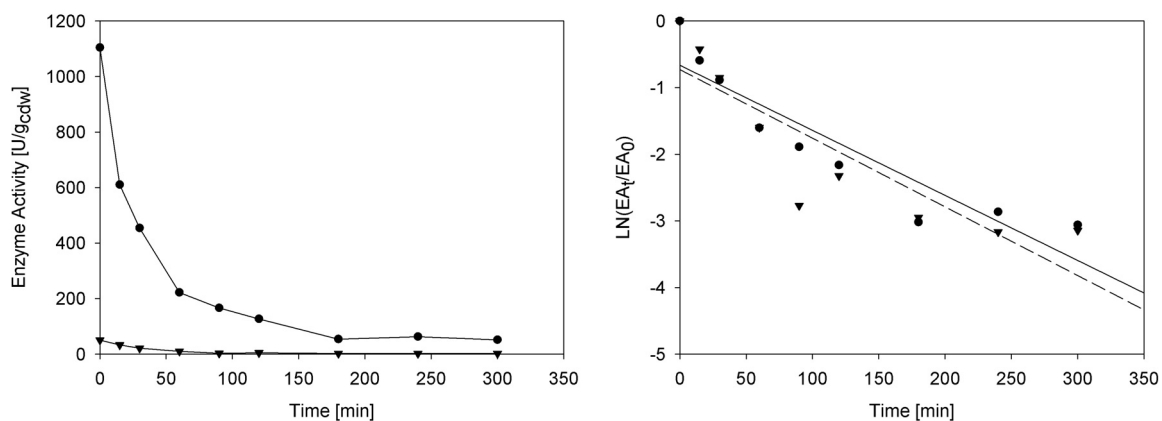


Figure 17. Half-life determination of XR- and FDH-activities in whole cell catalysts in the presence of 30 mM *o*-chloroacetophenone. Conditions: *E. coli* BL21 (DE3) pETDuet1_XR_FDHDH (whole cells); [cells] = 40 g_{CDW}/L; pH 7.5; 30°C; 30 rpm. Symbols: ● = XR, ▼ = FDH. XR-fit: $y = -0.0098x - 0.6642$; $R^2 = 0.848$. FDH-fit: $y = -0.0103x - 0.729$; $R^2 = 0.7694$.

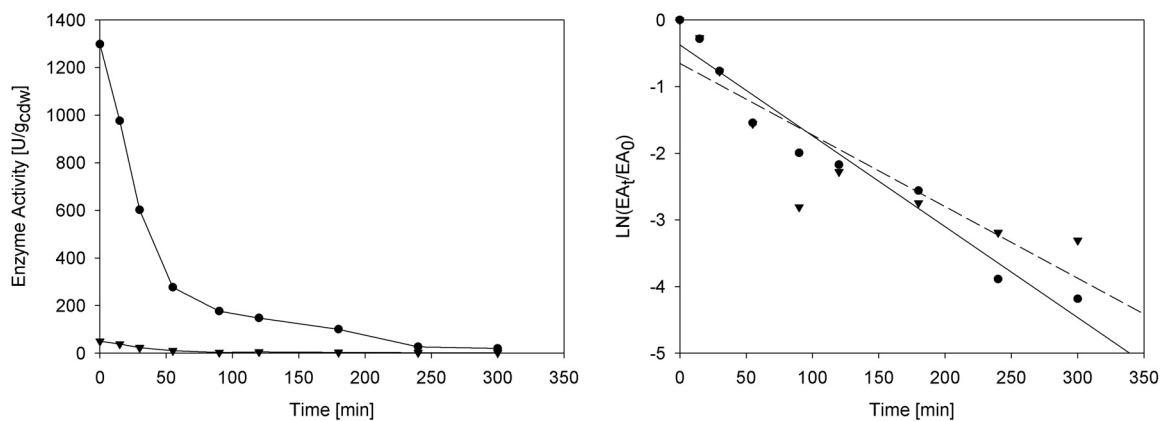


Figure 18. Half-life determination of XR- and FDH-activities in whole cell catalysts in the presence of 50 mM *o*-chloroacetophenone. Conditions: *E. coli* BL21 (DE3) pETDuet1_XR_FDHD (whole cells); [cells] = 40 g_{CDW}/L; pH 7.5; 30°C; 30 rpm. Symbols: ● = XR, ▼ = FDH. XR-fit: $y = -0.0136x - 0.3728$; $R^2 = 0.954$. FDH-fit: $y = -0.0107x - 0.6511$; $R^2 = 0.7894$.

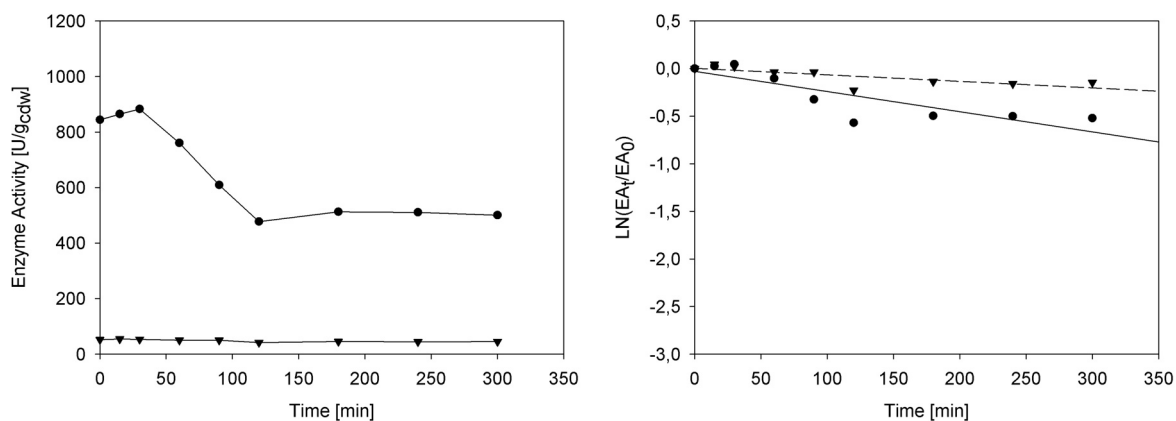


Figure 19. Half-life determination of XR- and FDH-activities in whole cell catalysts in the presence of 10 mM (S)-1-(2-chlorophenyl)ethanol. Conditions: *E. coli* BL21 (DE3) pETDuet1_XR_FDHD (whole cells); [cells] = 40 g_{CDW}/L; pH 7.5; 30°C; 30 rpm. Symbols: ● = XR, ▼ = FDH. XR-fit: $y = -0.0021x - 0.0287$; $R^2 = 0.7224$. FDH-fit: $y = -0.0007x + 0,003$; $R^2 = 0.58$.

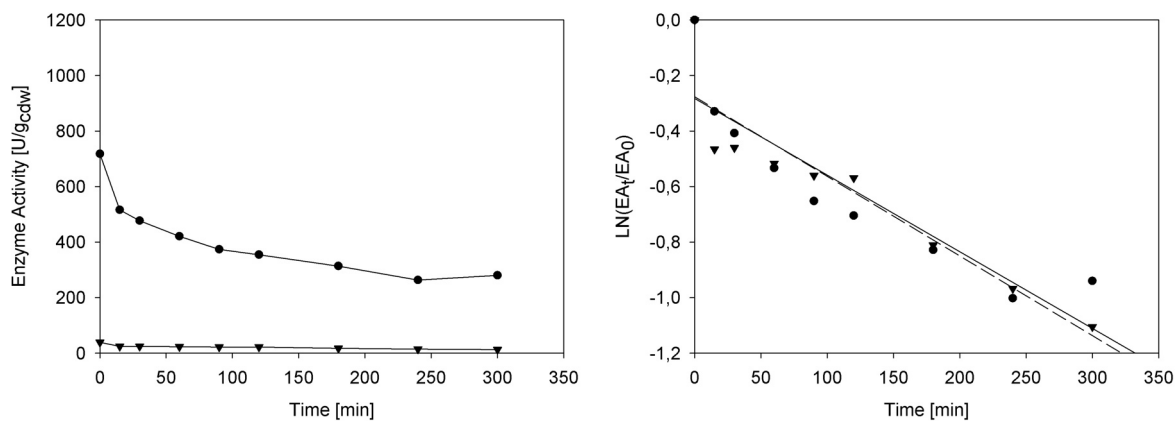


Figure 20. Half-life determination of XR- and FDH-activities in whole cell catalysts in the presence of 20 mM (S)-1-(2-chlorophenyl)ethanol. Conditions: *E. coli* BL21 (DE3) pETDuet1_XR_FDH (whole cells); [cells] = 40 g_{CDW}/L; pH 7.5; 30°C; 30 rpm. Symbols: ● = XR, ▼ = FDH. XR-fit: $y = -0.0028x - 0.2828$; $R^2 = 0.8205$. FDH-fit: $y = -0.0029x - 0.2765$; $R^2 = 0.8613$.

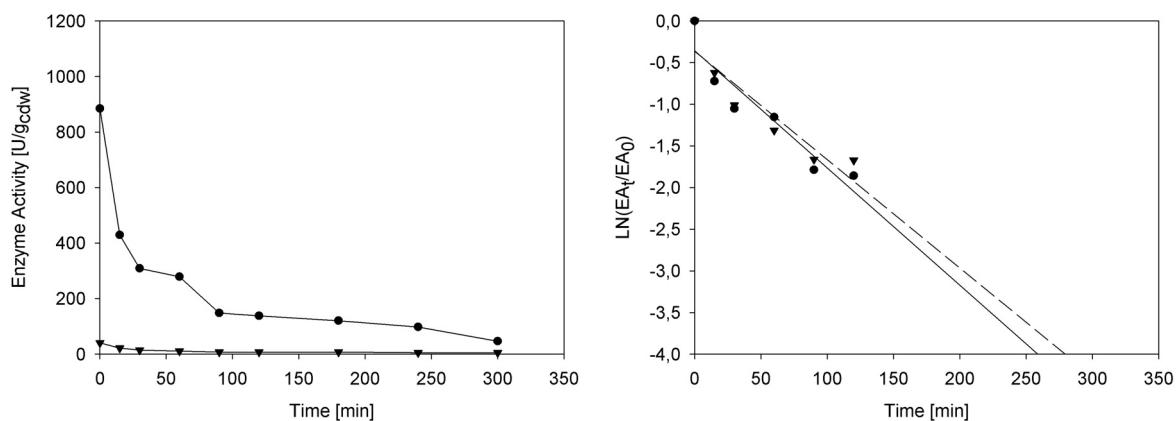


Figure 21. Half-life determination of XR- and FDH-activities in whole cell catalysts in the presence of 30 mM (S)-1-(2-chlorophenyl)ethanol. Conditions: *E. coli* BL21 (DE3) pETDuet1_XR_FDH (whole cells); [cells] = 40 g_{CDW}/L; pH 7.5; 30°C; 30 rpm. Symbols: ● = XR, ▼ = FDH. XR-fit: $y = -0.0141x - 0.3575$; $R^2 = 0.8793$. FDH-fit: $y = -0.013x - 0.364$; $R^2 = 0.8533$.

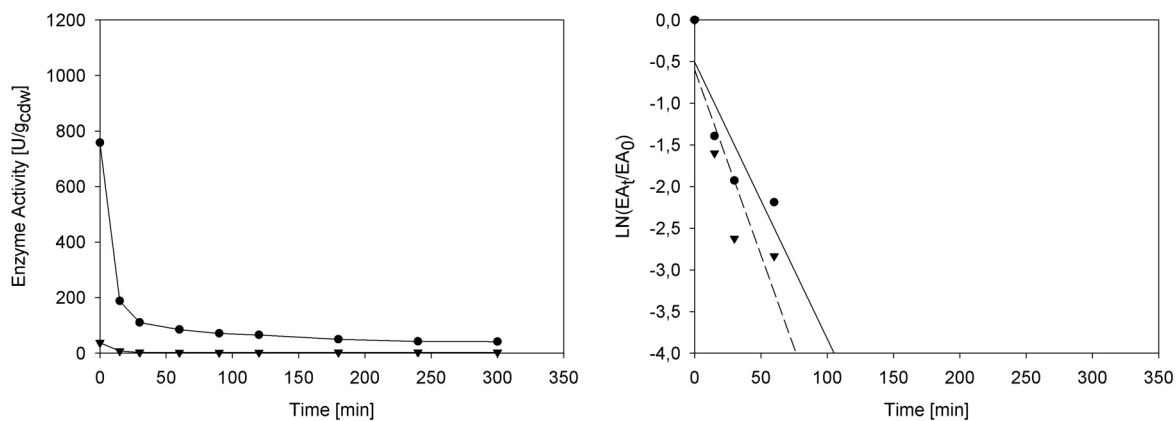


Figure 22. Half-life determination of XR- and FDH-activities in whole cell catalysts in the presence of 40 mM (S)-1-(2-chlorophenyl)ethanol. Conditions: *E. coli* BL21 (DE3) pETDuet1_XR_FDH (whole cells); [cells] = 40 g_{CDW}/L; pH 7.5; 30°C; 30 rpm. Symbols: ● = XR, ▼ = FDH. XR-fit: $y = -0.0332x - 0.5059$; $R^2 = 0.7599$. FDH-fit: $y = -0.0444x - 0.5974$; $R^2 = 0.7743$.

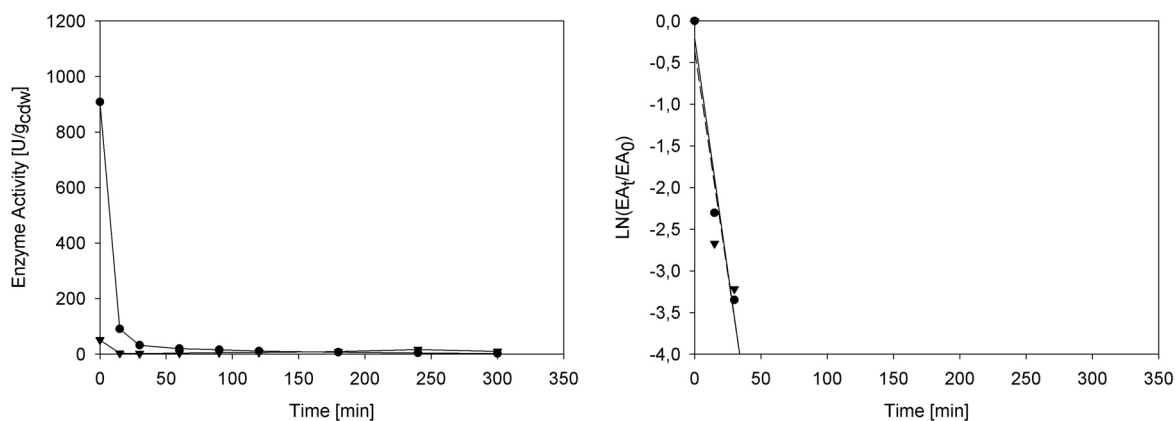


Figure 23. Half-life determination of XR- and FDH-activities in whole cell catalysts in the presence of 50 mM (S)-1-(2-chlorophenyl)ethanol (first measurement). Conditions: *E. coli* BL21 (DE3) pETDuet1_XR_FDH (whole cells); [cells] = 40 g_{CDW}/L; pH 7.5; 30°C; 30 rpm. Symbols: ● = XR, ▼ = FDH. XR-fit: $y = -0.1117x - 0.2098$; $R^2 = 0.955$. FDH-fit: $y = -0.1072x - 0,3546$; $R^2 = 0.8727$.

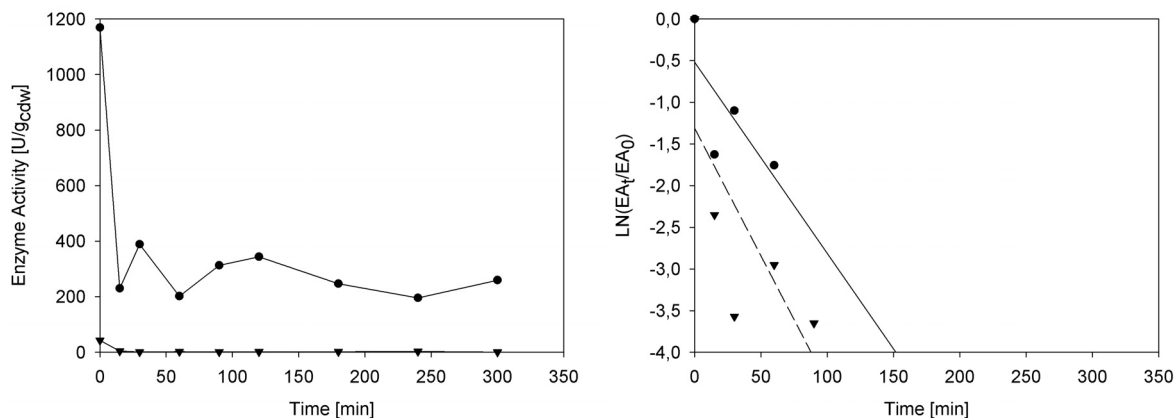


Figure 24. Half-life determination of XR- and FDH-activities in whole cell catalysts in the presence of 50 mM (*S*)-1-(2-chlorophenyl)ethanol (second measurement). Conditions: *E. coli* BL21 (DE3) pETDuet1_XR_FDHD (whole cells); [cells] = 40 g_{CDW}/L; pH 7.5; 30°C; 30 rpm. Symbols: ● = XR, ▼ = FDH. XR-fit: $y = -0.0229x - 0.5197$; $R^2 = 0.5393$. FDH-fit: $y = -0.0306x - 1.3124$; $R^2 = 0.5456$.

Table 3. Summary of XR and FDH half-life times in the presence of 0-50 mM *o*-chloroacetophenone.

Conc. [mM]	XR		FDH	
	λ [min ⁻¹]	$T_{1/2}$ [min]	λ [min ⁻¹]	$T_{1/2}$ [min]
0	-0.0001	6931	-0.00006	11552
3	-0.0001	6931	-0.00009	7702
6	-0.0002	3466	-0.0001	6931
10	-0.0009	770	-0.0014	495
20	-0.0062	112	-0.004	173
30	-0.0098	71	-0.0103	67
40	n.d.	n.d.	n.d.	n.d.
50	-0.0136	51	-0.0107	65

Table 4. Summary of XR and FDH half-life times in the presence of 0-50 mM (*S*)-1-(2-chlorophenyl)ethanol.

Conc. [mM]	XR		FDH	
	λ [min ⁻¹]	$T_{1/2}$ [min]	λ [min ⁻¹]	$T_{1/2}$ [min]
0	-0.0001	6931	-0.00006	11552
3	n.d.	n.d.	n.d.	n.d.
6	n.d.	n.d.	n.d.	n.d.
10	-0.0021	330	-0.0007	990
20	-0.0028	248	-0.0029	239
30	-0.0141	49	-0.013	53
40	-0.0332	21	-0,0444	16
50 ^{a)}	-0.0700	10	-0.0689	10

^{a)} Mean values of the 2 measurements

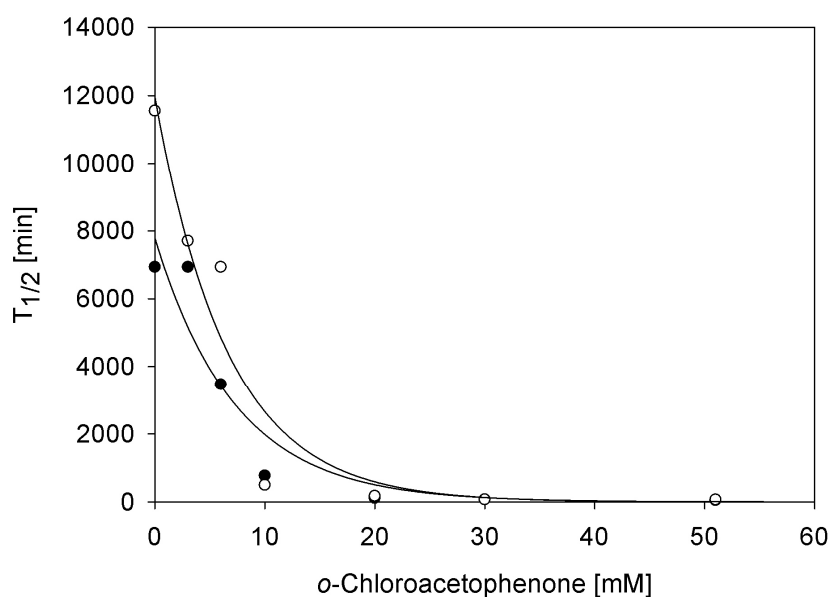


Figure 25. Dependence of XR and FDH half-life times on substrate concentration. Full circles are XR half-life times, open circles are FDH half-life times, solid lines are fits of the equation $y = a \cdot e^{-(b \cdot x)}$ to data points. XR-fit: R^2 : 0.9538; $a = 7786.0$; $b = 0.1368$. FDH-fit: R^2 : 0.9652; $a = 11952.0$; $b = 0.1504$. Conditions: *E. coli* BL21 (DE3) pETDuet1_XR_FDH (whole cells); [cells] = 40 g_{CDW}/L; pH 7.5; 30°C; 30 rpm.

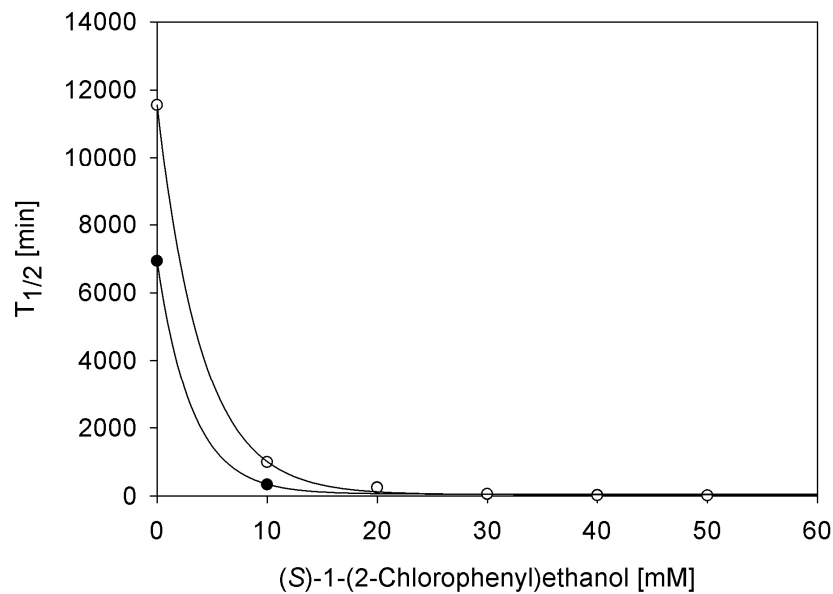


Figure 26. Dependence of XR and FDH half-life times on product concentration. Full circles are XR half-life times, open circles are FDH half-life times, solid lines are fits of the equation $y = y_0 + a \cdot e^{-(b \cdot x)}$ to data points. XR-fit: R^2 : 0.9995; $a = 6875.7$; $b = 0.3169$; $y_0 = 56.048$. FDH-fit: R^2 : 0.9999; $a = 11511.8$; $b = 0.2474$; $y_0 = 37.7830$. Conditions: *E. coli* BL21 (DE3) pETDuet1_XR_FDHDH (whole cells); [cells] = 40 g_{CDW}/L; pH 7.5; 30°C; 30 rpm.

B.2. Effect of Different *E. coli* Strains

We used *E. coli* BL21 (DE3) pETDuet1_XR_FDHD and *E. coli* Rosetta2 pETDuet1_XR_FDHD + pRSF_FDHD strains as catalysts in whole cell reductions. *E. coli* BL21 (DE3) pETDuet1_XR_FDHD carries pET-Duet-1 for co-expression of two genes, CtXR and CbFDH were cloned in the first and second multiple cloning site, respectively. *E. coli* Rosetta2 pETDuet1_XR_FDHD + pRSF_FDHD carries two additional plasmids, one that provides tRNAs for rare codons and a second high copy pRSF plasmid to increase the CbFDH gene copy number in the cell. *E. coli* Rosetta2 pETDuet1_XR_FDHD + pRSF_FDHD shows a 4-fold higher FDH-activity in the cell-free raw extract as compared to *E. coli* BL21 (DE3) pETDuet1_XR_FDHD (data shown in Master Thesis Katharina Mädje). Figure 27 and Figure 28 show vector maps of plasmids pETDuet-1 and pRSF-1b.

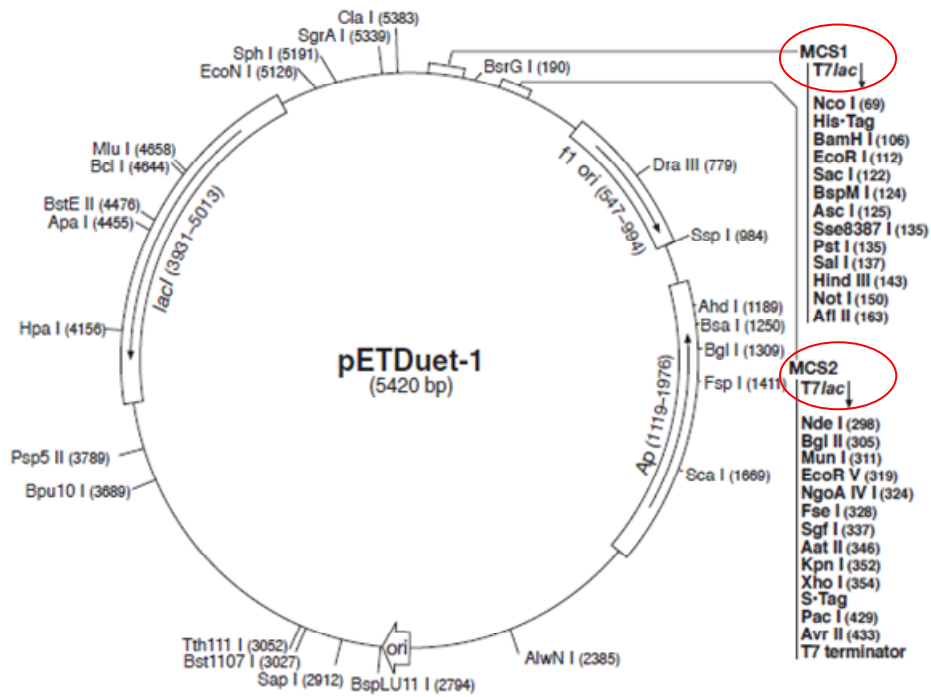


Figure 27. pETDuet-1 vector map. pETDuetTM-1 is designed for the co-expression of two target genes. The vector contains two multiple cloning sites (MCS), each of which is preceded by a T7 promoter/*lac* operator and a ribosome binding site (rbs). The vector also carries the pBR322-derived ColE1 replicon, *lacI* gene and ampicillin resistance gene.^[5]

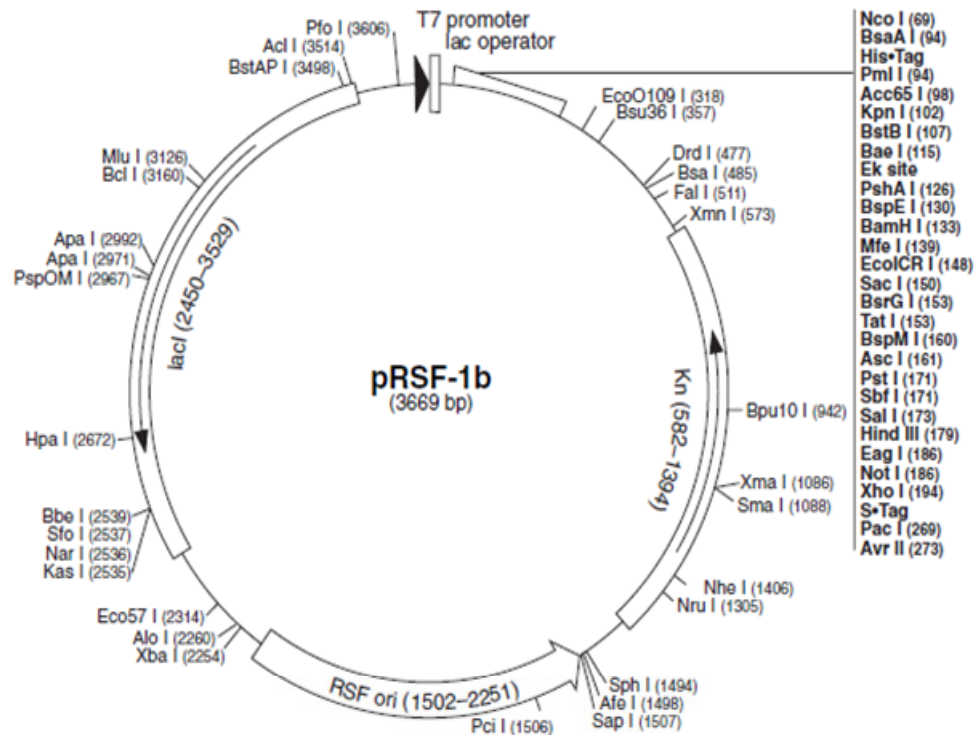


Figure 28. pRSF-1b vector map. pRSF-1b carries a T7 promoter and *lac* operator to control transcription, a replication origin derived from RSF1030, and kanamycin antibiotic resistance (KnR). It also encodes an N-terminal His•Tag® sequence followed by an enterokinase (Ek) cleavage site and an optional C-terminal S•Tag™ sequence. Unique sites are shown on the circle map. pRSF-1b is compatible with pET vectors (ColE1 origin), pCDF vectors (CloDF13 replication origin), and pACYC derived plasmids (P15A replication origin) carrying compatible antibiotic resistance markers.^[5]

B.3. Effect of pH

B.3.1. ISSS and ISPR by a Resin

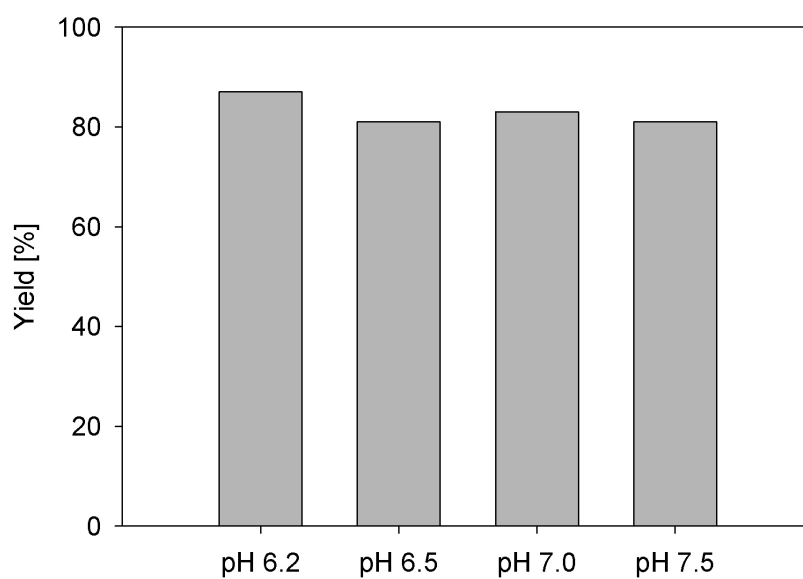


Figure 29. Chemical yield under different pH values in resin/water system. Reaction conditions: *E. coli* Rosetta2 pETDuet1_XR_FDHD + pRSF_FDHD; [cells] = 40 g_{CDW}/L; [substrate] = 100 mM; [resin] = 30 % (v/v); 30 °C; 30 rpm; 24 h.

B.3.2. ISSS and ISPR by Hexane

We performed additional two-phasic whole cell reductions (20 % v/v hexane) of 300 and 400 mM substrate in 100 mM potassium phosphate buffer, pH 6.2, supplemented with NAD⁺ (500 μ M) and polymyxin B sulphate (36 μ M). An analytical yield of 90 % was obtained in the experiment with 300 mM substrate at pH 6.2 as compared to 95 % at pH 6.5 (chapter 2.5.). The analytical yield in the bioreduction of 400 mM yielded 82 % product corresponding to 323 mM (Figure 30), which could not be enhanced by the use of higher hexane concentrations (Figure 31).

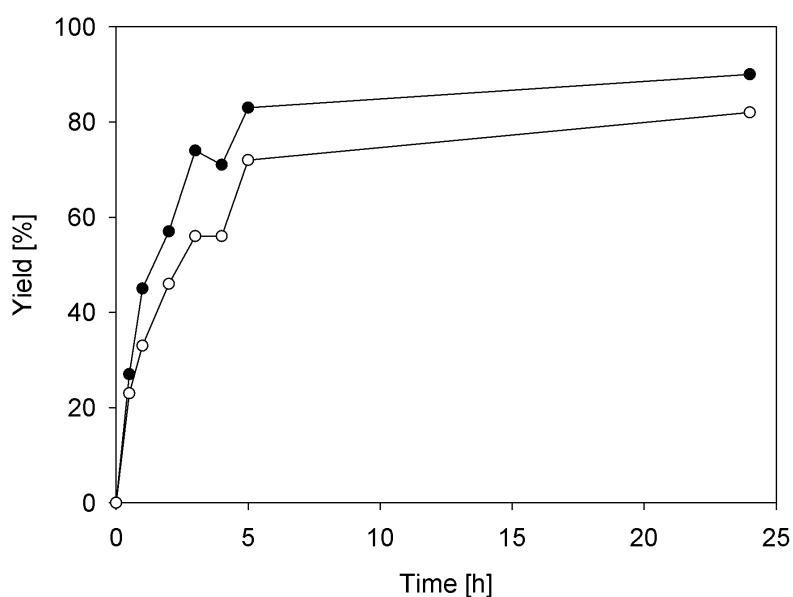


Figure 30. Time course of the *o*-chloroacetophenone reduction with hexane as co-solvent. Conditions: *E. coli* Rosetta2 pETDuet1_XR_FDHD + pRSF_FDHD (whole cells); [cells] = 40 g_{CDW}/L; pH 6.2; 30 °C; 30 rpm; + 20 vol% hexane. Symbols: ● = 300 mM *o*-chloroacetophenone; ○ = 400 mM *o*-chloroacetophenone.

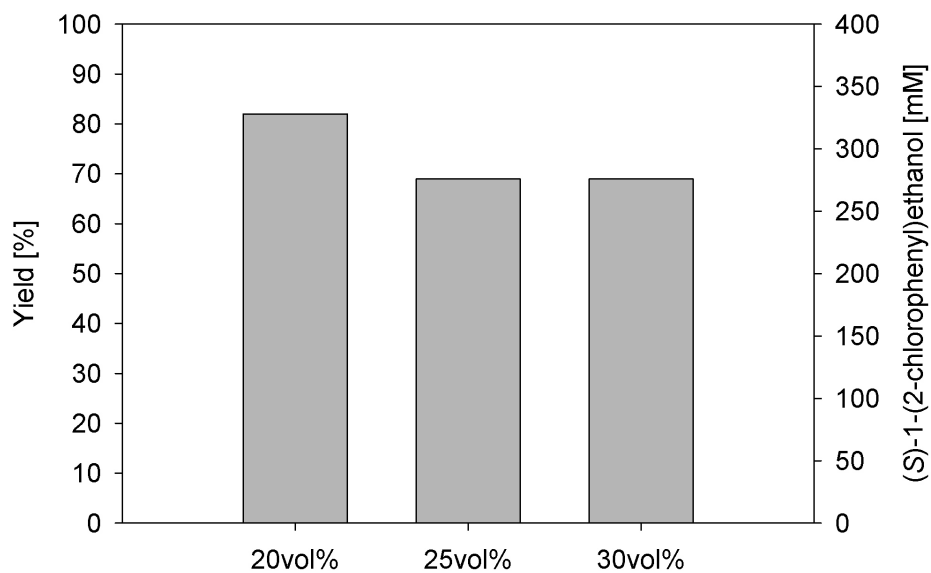


Figure 31. Determination of the optimal hexane concentration in the 400 mM o-chloroacetophenone conversion. Conditions: *E. coli* Rosetta2 pETDuet1_XR_FDHD + pRSF_FDHD (whole cells); [cells] = 40 g_{CDW}/L; [substrate] = 400 mM; pH 6.2; 30 °C; 30 rpm.

B.3.3. Substrate Toxicity at Different pH-values

Toxicity test with 30 mM *o*-chloroacetophenone was performed as described in chapter 2.2. Both enzymes (XR and FDH) had a 1.4-fold longer half-life when the potassium phosphate buffer pH 7.5 was replaced by a potassium phosphate buffer pH 6.2 (Figure 32 and Table 5).

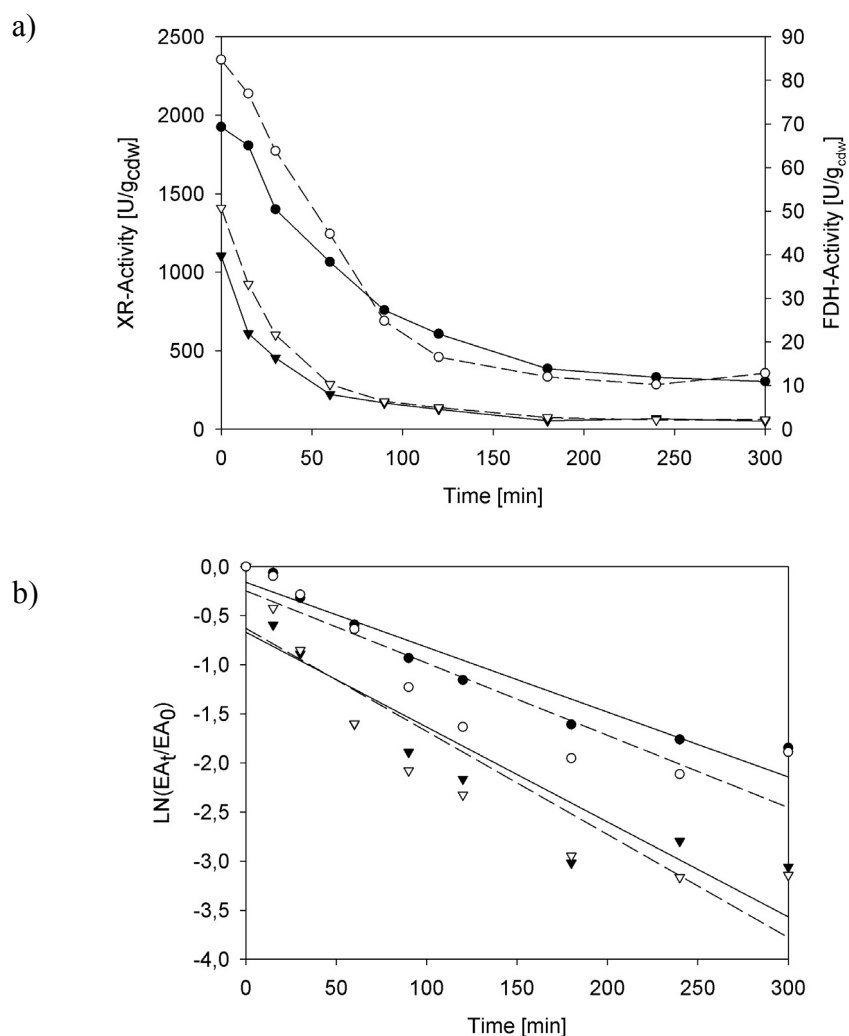


Figure 32. Half-life determination of XR- and FDH-activities in whole cell catalysts in the presence of 30 mM *o*-chloroacetophenone. Conditions: *E. coli* BL21 (DE3) pETDuet1_XR_FDH (whole cells); [cells] = 40 g_{CDW}/L; 30 °C; 30 rpm. Symbols: ● = XR pH 6.2; ○ = FDH pH 6.2; ▼ = XR pH 7.5; Δ = FDH pH 7.5. pH 6.2: XR-fit: $y = -0.0066x - 0.1596$; $R^2 = 0.929$; FDH-fit: $y = -0.0074x - 0.2464$; $R^2 = 0.8273$; pH 7.5: XR-fit: $y = -0.0097x - 0.6678$; $R^2 = 0.8433$; FDH-fit: $y = -0.0105x - 0.6294$; $R^2 = 0.8523$.

Table 5. Summary of XR and FDH half-life times in the presence of 30 mM *o*-chloroacetophenone at pH 7.5 and 6.2.

pH	XR		FDH	
	λ	$T_{1/2}$	λ	$T_{1/2}$
	[min ⁻¹]	[min]	[min ⁻¹]	[min]
7.5	-0.0097	71	-0.0105	66
6.2	-0.0066	105	-0.0074	94

B.4. Alternatives for Downstream-processing

Additional strategies for product isolation have been worked out in detail (Figure 33, Figure 34) but have not been tested.

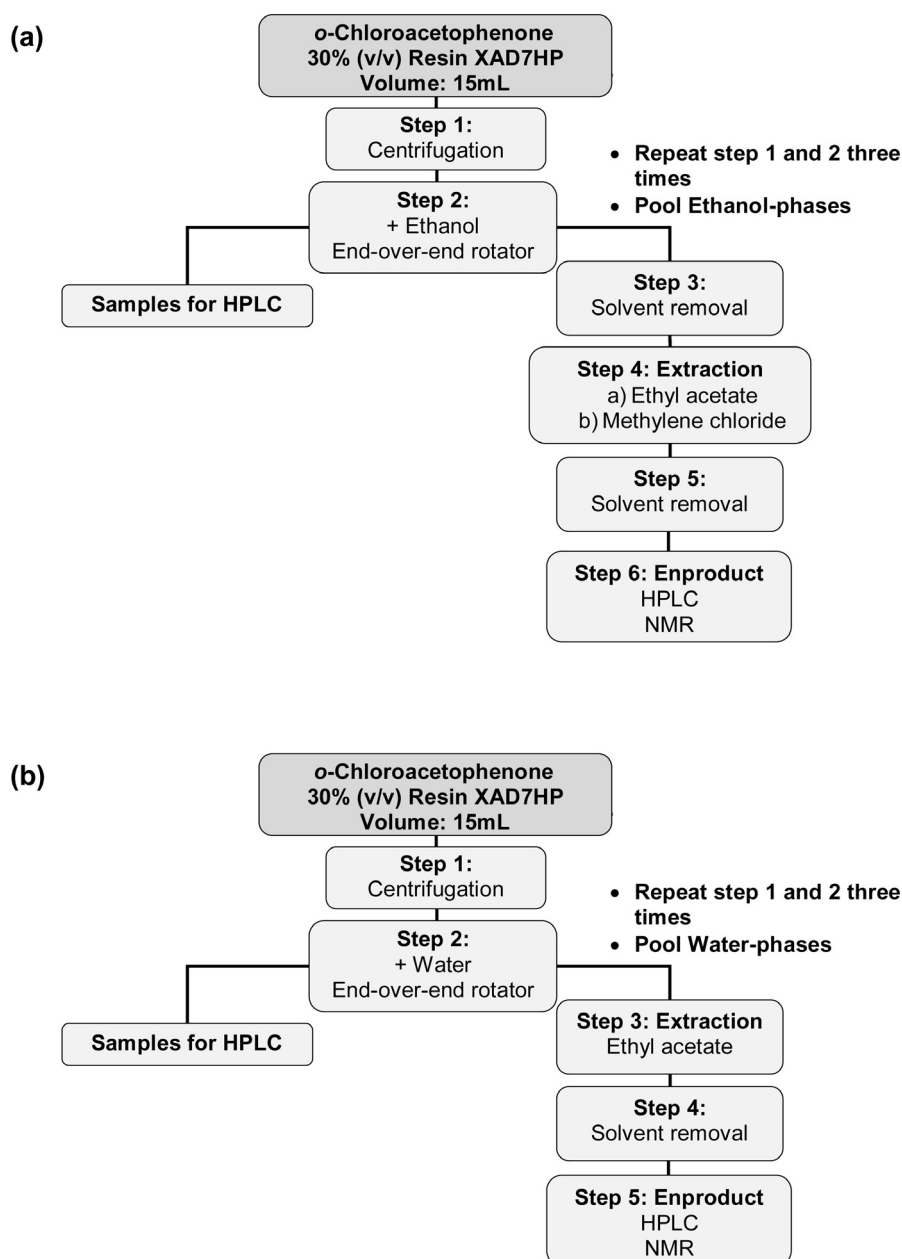


Figure 33. Two different strategies for product isolation in bioconversions with resin.

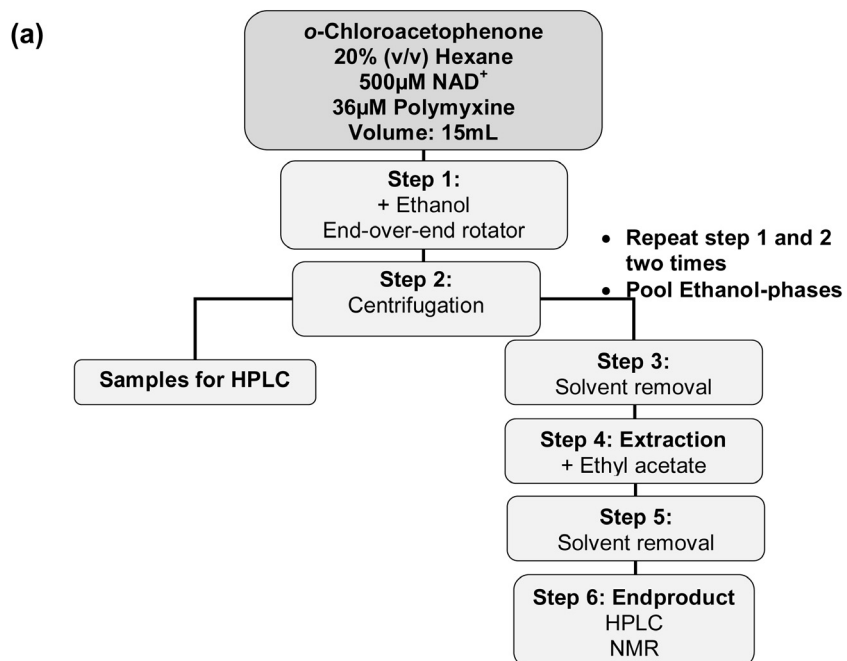


Figure 34. Strategy for product isolation in bioconversions with hexane as co-solvent.

B.5. NMR Spectra

^1H NMR spectra (Figure 35, Figure 36) were recorded on a DRX-400 Avance spectrometer (Bruker, Rheinstetten, Germany), equipped with an x-gradient inverse probe. ^1H irradiation and measurement frequency was 400.13 MHz, and the sample temperature was 300.2 K. All spectra were processed with the Topspin 1.3 software. Spectra were recorded with an acquisition of 32,768 data points, a relaxation delay of 1.0 s, and 64 scans. After zero filling to 65,536 data points the free induction decays were directly Fourier transformed to spectra with 8000 Hz (^1H). All spectra were recorded in CDCl_3 and referenced on internal CHCl_3 (δ ^1H : 7.24 ppm).

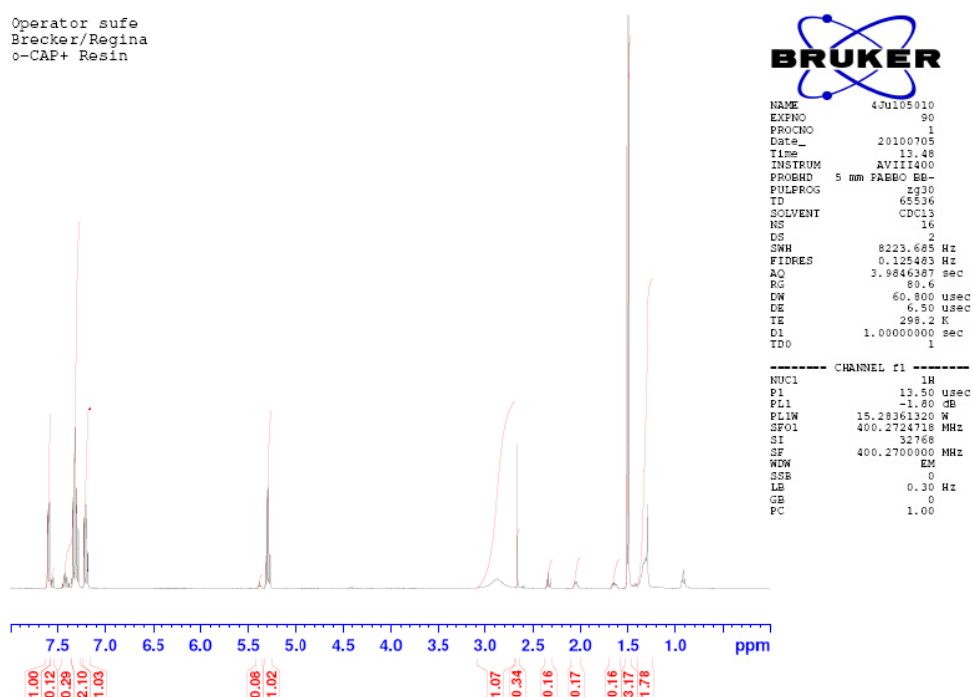


Figure 35. ^1H NMR spectra of the isolated product by scale-up experiment with 30 vol% resin (chapter 2.6.). Conditions: *E. coli* Rosetta2 pETDuet1_XR_FDHD + pRSF_FDHD (whole cells); Volume = 15 mL; pH 6.2; [cells] = 40 $\text{g}_{\text{CDW}}/\text{L}$; [o-chloroacetophenone] = 100 mM; Reaction time = 24 h.

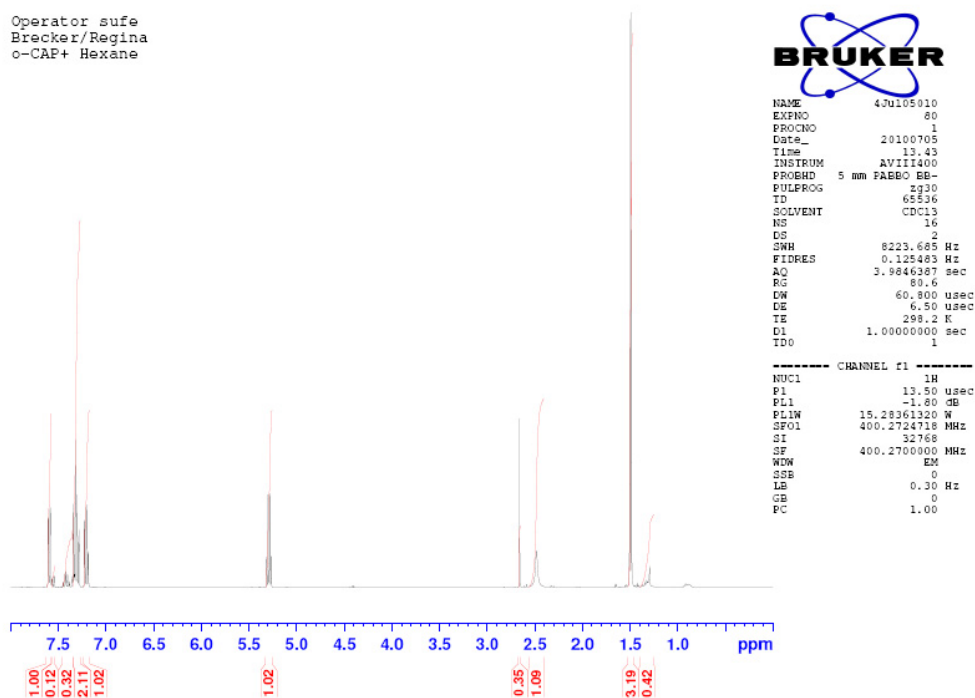


Figure 36. ^1H NMR spectra of the isolated product by scale-up experiment with 20 vol% hexane (chapter 2.6). Conditions: *E. coli* Rosetta2 pETDuet1_XR_FDHD + pRSF_FDHD (whole cells); Volume = 15 mL; pH 6.2; [cells] = 40 g_{CDW}/L; [*o*-chloroacetophenone] = 300 mM; [NAD⁺] = 500 mM; [polymyxine B sulphate] = 36 μM ; Reaction time = 24 h.

Both spectra show a lot of product, but regardless of the second phase (resin or hexane), there are still ~ 12 % substrate and other contaminants left.

C. Registers

C.1. Register of Figures

Figure 1. Time course of resin-based whole cell bioreductions using 100 mM substrate and 20 vol% resin. Conditions: *E. coli* BL21 (DE3) pETDuet1_XR_FDHD (whole cells); [cells] = 40 g_{CDW}/L; pH 7.5; 30°C; 30 rpm. Symbols: ● = 100 mM *o*-chloroacetophenone + 20 vol% resin..... 17

Figure 2. Time courses of resin-based whole cell bioreductions varying substrate and resin concentrations. Conditions: *E. coli* BL21 (DE3) pETDuet1_XR_FDHD (whole cells); [cells] = 40 g_{CDW}/L; pH 7.5; 30°C; 30 rpm. Symbols: ● = 100 mM *o*-chloroacetophenone + 30 vol% resin; ○ = 100 mM *o*-chloroacetophenone + 40 vol% resin; ▼ = 100 mM *o*-chloroacetophenone + 35 vol% resin; Δ = 200 mM *o*-chloroacetophenone + 60 vol% resin..... 17

Figure 3. Effects of externally added NAD⁺ and cell permeabilization on resin-based, whole cell bioreductions of *o*-chloroacetophenone. Conditions: *E. coli* BL21 (DE3) pETDuet1_XR_FDHD (whole cells); [cells] = 40 g_{CDW}/L; [substrate] = 100 mM; pH 7.5; 30°C; 30 rpm. Symbols: ● = + 30 vol% resin; ○ = + 30 vol% resin + NAD⁺ [500 μM]; ▼ = + 30 vol% resin + NAD⁺ [500 μM] + polymyxin B sulphate [36 μM]..... 19

Figure 4. Effects of co-solvent amount and type on whole cell bioreduction rates of *o*-chloroacetophenone. Conditions: *E. coli* BL21 (DE3) pETDuet1_XR_FDHD (whole cells); [cells] = 40 g_{CDW}/L; [substrate] = 100 mM; pH 7.5; 30°C; 30 rpm. Symbols: ● = + 20 vol% hexane; ○ = + 50 vol% hexane; ▼ = + 20 vol% heptane; Δ = + 50 vol% heptane; ■ = + 20 vol% dodecane; □ = + 50 vol% dodecane; ◆ = + 20 vol% BMIMPF₆; ◇ = + 50 vol% BMIMPF₆..... 21

Figure 5. Optimization of 100 mM *o*-chloroacetophenone reduction by *E. coli* BL21 (DE3) pETDuet1_XR_FDHD (whole cells). The effects of organic co-solvents, cell permeabilization and externally added NAD⁺ on yields. Conditions: [cells] = 40 g_{CDW}/L; [substrate] = 100 mM; [co-solvents] = 20 vol%; reaction time 24 h; pH 7.5; 30°C; 30 rpm. Black bars: experiment with co-solvent; Grey bars: with additional NAD⁺ [0.5 mM]; Dark grey bars: with additional NAD⁺ [500 μM] and polymyxin B sulphate [36 μM]. I.L. = ionic liquid (BMIMPF₆)..... 22

Figure 6. Optimization of the 200 mM *o*-chloroacetophenone reduction. The effects of different co-solvent concentrations on yields. Conditions: *E. coli* BL21 (DE3) pETDuet1_XR_FDHD (whole cells); [cells] = 40 g_{CDW}/L; [substrate] = 200 mM; pH 7.5; 30°C; 30 rpm. Symbols: ● = + 20 vol% hexane; ○ = + 20 vol% hexane + NAD⁺ (500μM) + PM (50mg/L); ▼ = + 30 vol% hexane; Δ = + 30 vol% hexane + NAD⁺ (500μM) + PM (50mg/L); ■ = + 40 vol% hexane; □ = + 40 vol% hexane + NAD⁺ (500μM) + PM (50mg/L)..... 23

Figure 7. Comparison of *o*-chloroacetophenone reduction with two different whole-cell catalysts. Conditions: [cells] = 40 g_{CDW}/L; [substrate] = 200 mM; [hexane] = 20 % (v/v); [NAD⁺] = 500 μM; [polymyxin B sulphate] = 36 μM; pH 7.5; 30°C; 30 rpm. Symbols: ● = *E. coli* Rosetta2 pETDuet1_XR_FDHD + pRSF_FDHD; ○ = *E. coli* BL21 (DE3) pETDuet1_XR_FDHD..... 25

Figure 8. Effect of different pH-values on XR- and FDH-activity and corresponding chemical yields. Reaction conditions: *E. coli* Rosetta2 pETDuet1_XR_FDHD + pRSF_FDHD; Conversion: [cells] = 40 g_{CDW}/L; 30°C; 30 rpm; 24 h. (a) [substrate] = 100 mM, (b) [substrate] = 200 mM. Enzyme-activity: crude cell extract, [xylose] = 700 mM; [sodium formate] = 200 mM; reaction time = 5 min; 25°C; ● = XR; ○ = FDH. 27

- Figure 9. Chemical yield under different pH values in hexane/water system. Conditions: *E. coli* Rosetta2 pETDuet1_XR_FDHD + pRSF_FDHD; [cells] = 40 g_{CDW}/L; [substrate] = 200 mM; [hexane] = 20 % (v/v); 30°C; 30 rpm; 24 h..... 28
- Figure 10. Setup for the scale-up experiments with (a) resin or (b) hexane and the schematic view of the downstream-processing. Conditions: *E. coli* Rosetta2 pETDuet1_XR_FDHD + pRSF_FDHD (whole cells); [cells] = 40 g_{CDW}/L; Reaction time = 24 h. 30
- Figure 11. Imidazopyridine PLK1 inhibitor example with good anti-tumor efficacy. 41
- Figure 12. Half-life determination of XR- and FDH-activities in whole cell catalysts in the presence of 0 mM *o*-chloroacetophenone and 0 mM (*S*)-1-(2-chlorophenyl)ethanol. Conditions: *E. coli* BL21 (DE3) pETDuet1_XR_FDHD (whole cells); [cells] = 40 g_{CDW}/L; pH 7.5; 30°C; 30 rpm. Symbols: ● = XR, ▼ = FDH. XR-fit: $y = -0.0001x - 0.4229$; $R^2 = 0.8552$. FDH-fit: $y = -6E-05x - 0.2727$; $R^2 = 0.6375$ 43
- Figure 13. Half-life determination of XR- and FDH-activities in whole cell catalysts in the presence of 3 mM *o*-chloroacetophenone. Conditions: *E. coli* BL21 (DE3) pETDuet1_XR_FDHD (whole cells); [cells] = 40 g_{CDW}/L; pH 7.5; 30°C; 30 rpm. Symbols: ● = XR, ▼ = FDH. XR-fit: $y = -0.0001x - 0.5922$; $R^2 = 0.8909$. FDH-fit: $y = -9E-05x - 0.3193$; $R^2 = 0.755$ 43
- Figure 14. Half-life determination of XR- and FDH-activities in whole cell catalysts in the presence of 6 mM *o*-chloroacetophenone. Conditions: *E. coli* BL21 (DE3) pETDuet1_XR_FDHD (whole cells); [cells] = 40 g_{CDW}/L; pH 7.5; 30°C; 30 rpm. Symbols: ● = XR, ▼ = FDH. XR-fit: $y = -0.0002x - 1.2336$; $R^2 = 0.8848$. FDH-fit: $y = -0.0001x - 0.7768$; $R^2 = 0.8467$ 44
- Figure 15. Half-life determination of XR- and FDH-activities in whole cell catalysts in the presence of 10 mM *o*-chloroacetophenone. Conditions: *E. coli* BL21 (DE3)

pETDuet1_XR_FDH (whole cells); [cells] = 40 g_{CDW}/L; pH 7.5; 30°C; 30 rpm. Symbols: ● = XR, ▼ = FDH. XR-fit: $y = -0.0009x - 0.0098$; $R^2 = 0.7543$. FDH-fit: $y = -0.0014x + 0.0356$; $R^2 = 0.8665$ 44

Figure 16. Half-life determination of XR- and FDH-activities in whole cell catalyts in the presence of 20 mM *o*-chloroacetophenone. Conditions: *E. coli* BL21 (DE3)

pETDuet1_XR_FDH (whole cells); [cells] = 40 g_{CDW}/L; pH 7.5; 30°C; 30 rpm. Symbols: ● = XR, ▼ = FDH. XR-fit: $y = -0.0062x - 0.2202$; $R^2 = 0.8628$. FDH-fit: $y = -0.004x - 0.2424$; $R^2 = 0.9214$ 45

Figure 17. Half-life determination of XR- and FDH-activities in whole cell catalyts in the presence of 30 mM *o*-chloroacetophenone. Conditions: *E. coli* BL21 (DE3)

pETDuet1_XR_FDH (whole cells); [cells] = 40 g_{CDW}/L; pH 7.5; 30°C; 30 rpm. Symbols: ● = XR, ▼ = FDH. XR-fit: $y = -0.0098x - 0.6642$; $R^2 = 0.848$. FDH-fit: $y = -0.0103x - 0.729$; $R^2 = 0.7694$ 45

Figure 18. Half-life determination of XR- and FDH-activities in whole cell catalyts in the presence of 50 mM *o*-chloroacetophenone. Conditions: *E. coli* BL21 (DE3)

pETDuet1_XR_FDH (whole cells); [cells] = 40 g_{CDW}/L; pH 7.5; 30°C; 30 rpm. Symbols: ● = XR, ▼ = FDH. XR-fit: $y = -0.0136x - 0.3728$; $R^2 = 0.954$. FDH-fit: $y = -0.0107x - 0.6511$; $R^2 = 0.7894$ 46

Figure 19. Half-life determination of XR- and FDH-activities in whole cell catalyts in the presence of 10 mM (*S*)-1-(2-chlorophenyl)ethanol. Conditions: *E. coli* BL21 (DE3)

pETDuet1_XR_FDH (whole cells); [cells] = 40 g_{CDW}/L; pH 7.5; 30°C; 30 rpm. Symbols: ● = XR, ▼ = FDH. XR-fit: $y = -0.0021x - 0.0287$; $R^2 = 0.7224$. FDH-fit: $y = -0.0007x + 0.003$; $R^2 = 0.58$ 46

Figure 20. Half-life determination of XR- and FDH-activities in whole cell catalysts in the presence of 20 mM (*S*)-1-(2-chlorophenyl)ethanol. Conditions: *E. coli* BL21 (DE3) pETDuet1_XR_FDH (whole cells); [cells] = 40 g_{CDW}/L; pH 7.5; 30°C; 30 rpm. Symbols: ● = XR, ▼ = FDH. XR-fit: $y = -0.0028x - 0.2828$; $R^2 = 0.8205$. FDH-fit: $y = -0.0029x - 0.2765$; $R^2 = 0.8613$ 47

Figure 21. Half-life determination of XR- and FDH-activities in whole cell catalysts in the presence of 30 mM (*S*)-1-(2-chlorophenyl)ethanol. Conditions: *E. coli* BL21 (DE3) pETDuet1_XR_FDH (whole cells); [cells] = 40 g_{CDW}/L; pH 7.5; 30°C; 30 rpm. Symbols: ● = XR, ▼ = FDH. XR-fit: $y = -0.0141x - 0.3575$; $R^2 = 0.8793$. FDH-fit: $y = -0.013x - 0.364$; $R^2 = 0.8533$ 47

Figure 22. Half-life determination of XR- and FDH-activities in whole cell catalysts in the presence of 40 mM (*S*)-1-(2-chlorophenyl)ethanol. Conditions: *E. coli* BL21 (DE3) pETDuet1_XR_FDH (whole cells); [cells] = 40 g_{CDW}/L; pH 7.5; 30°C; 30 rpm. Symbols: ● = XR, ▼ = FDH. XR-fit: $y = -0.0332x - 0.5059$; $R^2 = 0.7599$. FDH-fit: $y = -0.0444x - 0.5974$; $R^2 = 0.7743$ 48

Figure 23. Half-life determination of XR- and FDH-activities in whole cell catalysts in the presence of 50 mM (*S*)-1-(2-chlorophenyl)ethanol (first measurement). Conditions: *E. coli* BL21 (DE3) pETDuet1_XR_FDH (whole cells); [cells] = 40 g_{CDW}/L; pH 7.5; 30°C; 30 rpm. Symbols: ● = XR, ▼ = FDH. XR-fit: $y = -0.1117x - 0.2098$; $R^2 = 0.955$. FDH-fit: $y = -0.1072x - 0,3546$; $R^2 = 0.8727$ 48

Figure 24. Half-life determination of XR- and FDH-activities in whole cell catalysts in the presence of 50 mM (*S*)-1-(2-chlorophenyl)ethanol (second measurement). Conditions: *E. coli* BL21 (DE3) pETDuet1_XR_FDH (whole cells); [cells] = 40 g_{CDW}/L; pH 7.5; 30°C;

30 rpm. Symbols: ● = XR, ▼ = FDH. XR-fit: $y = -0.0229x - 0.5197$; $R^2 = 0.5393$. FDH-fit: $y = -0.0306x - 1.3124$; $R^2 = 0.5456$ 49

Figure 25. Dependence of XR and FDH half-life times on substrate concentration. Full circles are XR half-life times, open circles are FDH half-life times, solid lines are fits of the equation $y = a \cdot e^{-(b \cdot x)}$ to data points. XR-fit: $R^2: 0.9538$; $a = 7786.0$; $b = 0.1368$. FDH-fit: $R^2: 0.9652$; $a = 11952.0$; $b = 0.1504$. Conditions: *E. coli* BL21 (DE3) pETDuet1_XR_FDH (whole cells); [cells] = 40 g_{CDW}/L; pH 7.5; 30°C; 30 rpm. 50

Figure 26. Dependence of XR and FDH half-life times on product concentration. Full circles are XR half-life times, open circles are FDH half-life times, solid lines are fits of the equation $y = y_0 + a \cdot e^{-(b \cdot x)}$ to data points. XR-fit: $R^2: 0.9995$; $a = 6875.7$; $b = 0.3169$; $y_0 = 56.048$. FDH-fit: $R^2: 0.9999$; $a = 11511.8$; $b = 0.2474$; $y_0 = 37.7830$. Conditions: *E. coli* BL21 (DE3) pETDuet1_XR_FDH (whole cells); [cells] = 40 g_{CDW}/L; pH 7.5; 30°C; 30 rpm. 51

Figure 27. pETDuet-1 vector map. pETDuetTM-1 is designed for the co-expression of two target genes. The vector contains two multiple cloning sites (MCS), each of which is preceded by a T7 promoter/*lac* operator and a ribosome binding site (rbs). The vector also carries the pBR322-derived ColE1 replicon, *lacI* gene and ampicillin resistance gene.^[5] 53

Figure 28. pRSF-1b vector map. pRSF-1b carries a T7 promoter and *lac* operator to control transcription, a replication origin derived from RSF1030, and kanamycin antibiotic resistance (KnR). It also encodes an N-terminal His•Tag® sequence followed by an enterokinase (Ek) cleavage site and an optional C-terminal S•TagTM sequence. Unique sites are shown on the circle map. pRSF-1b is compatible with pET vectors (ColE1

- origin), pCDF vectors (CloDF13 replication origin), and pACYC derived plasmids (P15A replication origin) carrying compatible antibiotic resistance markers.^[5] 54
- Figure 29. Chemical yield under different pH values in resin/water system. Reaction conditions: *E. coli* Rosetta2 pETDuet1_XR_FDHD + pRSF_FDHD; [cells] = 40 g_{CDW}/L; [substrate] = 100 mM; [resin] = 30 % (v/v); 30 °C; 30 rpm; 24 h. 55
- Figure 30. Time course of the *o*-chloroacetophenone reduction with hexane as co-solvent. Conditions: *E. coli* Rosetta2 pETDuet1_XR_FDHD + pRSF_FDHD (whole cells); [cells] = 40 g_{CDW}/L; pH 6.2; 30 °C; 30 rpm; + 20 vol% hexane. Symbols: ● = 300 mM *o*-chloroacetophenone; ○ = 400 mM *o*-chloroacetophenone. 56
- Figure 31. Determination of the optimal hexane concentration in the 400 mM *o*-chloroacetophenone conversion. Conditions: *E. coli* Rosetta2 pETDuet1_XR_FDHD + pRSF_FDHD (whole cells); [cells] = 40 g_{CDW}/L; [substrate] = 400 mM; pH 6.2; 30 °C; 30 rpm. 57
- Figure 32. Half-life determination of XR- and FDH-activities in whole cell catalysts in the presence of 30 mM *o*-chloroacetophenone. Conditions: *E. coli* BL21 (DE3) pETDuet1_XR_FDHD (whole cells); [cells] = 40 g_{CDW}/L; 30 °C; 30 rpm. Symbols: ● = XR pH 6.2; ○ = FDH pH 6.2; ▼ = XR pH 7.5; Δ = FDH pH 7.5. pH 6.2: XR-fit: $y = -0.0066x - 0.1596$; $R^2 = 0.929$; FDH-fit: $y = -0.0074x - 0.2464$; $R^2 = 0.8273$; pH 7.5: XR-fit: $y = -0.0097x - 0.6678$; $R^2 = 0.8433$; FDH-fit: $y = -0.0105x - 0.6294$; $R^2 = 0,8523$. 58
- Figure 33. Two different strategies for product isolation in bioconversions with resin. 60
- Figure 34. Strategy for product isolation in bioconversions with hexane as co-solvent. 61
- Figure 35. ¹H NMR spectra of the isolated product by scale-up experiment with 30 vol% resin (chapter 2.6.). Conditions: *E. coli* Rosetta2 pETDuet1_XR_FDHD + pRSF_FDHD (whole

cells); Volume = 15 mL; pH 6.2; [cells] = 40 g_{CDW}/L; [*o*-chloroacetophenone] = 100 mM; Reaction time = 24 h..... 62

Figure 36. ¹H NMR spectra of the isolated product by scale-up experiment with 20 vol% hexane (chapter 2.6.). Conditions: *E. coli* Rosetta2 pETDuet1_XR_FDHD + pRSF_FDHD (whole cells); Volume = 15 mL; pH 6.2; [cells] = 40 g_{CDW}/L; [*o*-chloroacetophenone] = 300 mM; [NAD⁺] = 500 mM; [polymyxine B sulphate] = 36 μM; Reaction time = 24 h. 63

C.2. Register of Schemes

Scheme 1. Whole-cell biocatalytic reduction of <i>o</i> -chloroacetophenone using recombinant <i>E.coli</i> strains co-expressing <i>Candida tenuis</i> xylose reductase (<i>CtXR</i>) and <i>Candida boidinii</i> formate dehydrogenase (<i>CbFDH</i>).....	11
--	----

C.3. Register of Tables

Table 1. Effect of substrate (end)-concentration and feeding rate on yields in batch and fed-batch conversions of <i>o</i> -chloroacetophenone with <i>E. coli</i> BL21 (DE3) pETDuet1_XR_FDH. ^{a)}	13
Table 2. Half-life of the enzymes XR and FDH in the presence of different substrate and product concentrations. ^{a)}	14
Table 3. Summary of XR and FDH half-life times in the presence of 0-50 mM <i>o</i> -chloroacetophenone.....	49
Table 4. Summary of XR and FDH half-life times in the presence of 0-50 mM (<i>S</i>)-1-(2-chlorophenyl)ethanol.....	50
Table 5. Summary of XR and FDH half-life times in the presence of 30 mM <i>o</i> -chloroacetophenone at pH 7.5 and 6.2.	59

D. References Appendix

- [1] Y. Sato, Y. Onozaki, T. Sugimoto, H. Kurihara, K. Kamijo, C. Kadowaki, T. Tsujino, A. Watanabe, S. Otsuki, M. Mitsuya, M. Iida, K. Haze, T. Machida, Y. Nakatsuru, H. Komatani, H. Kotani, Y. Iwasawa, *Bioorg. Med. Chem. Lett.* **2009**, *19*, 4673-4678.
- [2] T. R. Rheault, M. Cheung, J. G. B. Alberti, K. H. Donaldson, *PCT Int. Appl.* **2008**, WO 2008070354 A2 20080612.
- [3] T. Stengel, M. Schmidt, S. Weinbrenner, A. Weber, P. Gimmich, V. Gekeler, T. Beckers, A. Zimmermann, T. Maier, B. Schmidt, F. Dehmel, *PCT Int. Appl.* **2009**, WO 2009003911 A1 20090108.
- [4] A. Santamaria, R. Neef, U. Eberspächer, K. Eis, M. Husemann, D. Mumberg, S. Prechtel, V. Schulze, G. Siemeister, L. Wortmann, F. A. Barr, E. A. Nigg, *Mol. Biol. Cell.* **2007**, *18*, 4024-4036.
- [5] <http://www.emdchemicals.com/>